NSF | NCAR OPERATED BY UCAR | High Altitude Observatory

May 13, 2026

Tomographic Reconstructions of Coronal Mass Ejections
with Physics-Informed Neural Radiance Fields

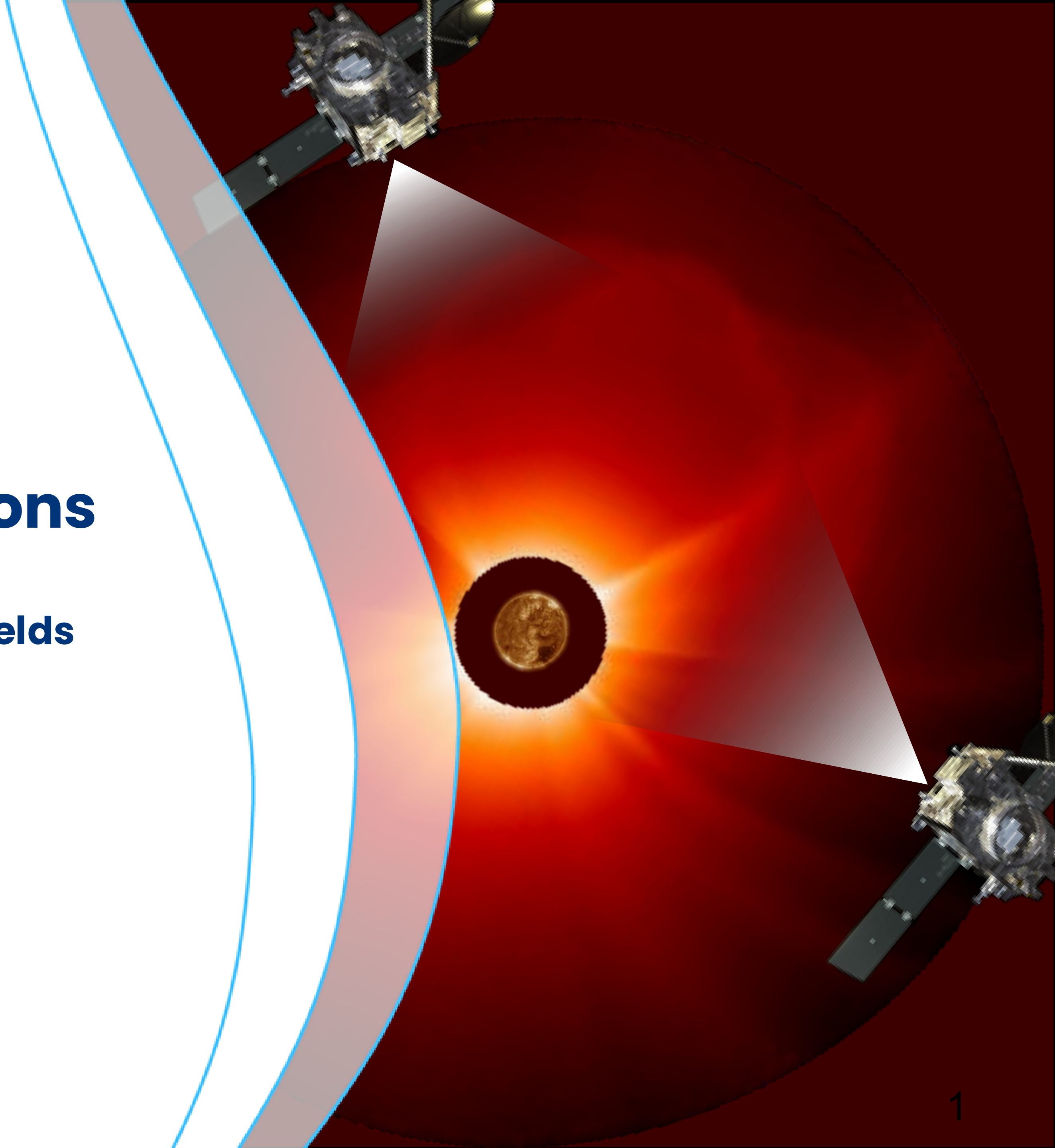

Robert Jarolim
NASA Jack Eddy Fellow
PUNCH Associate Investigator
High Altitude Observatory

CPAESS NASA

This material is based upon work supported by the NSF National Center for Atmospheric Research, a major facility sponsored by the U.S. National Science Foundation and managed by the University Corporation for Atmospheric Research. Any opinions, findings and conclusions or recommendations expressed in this material do not necessarily reflect the views of NSF.

Observing capabilities for Coronal Mass Ejections (CMEs)

- **Estimation of 3D structures from 2D images is challenging**
  - **optically-thin plasma**
  - **Thomson scattering**

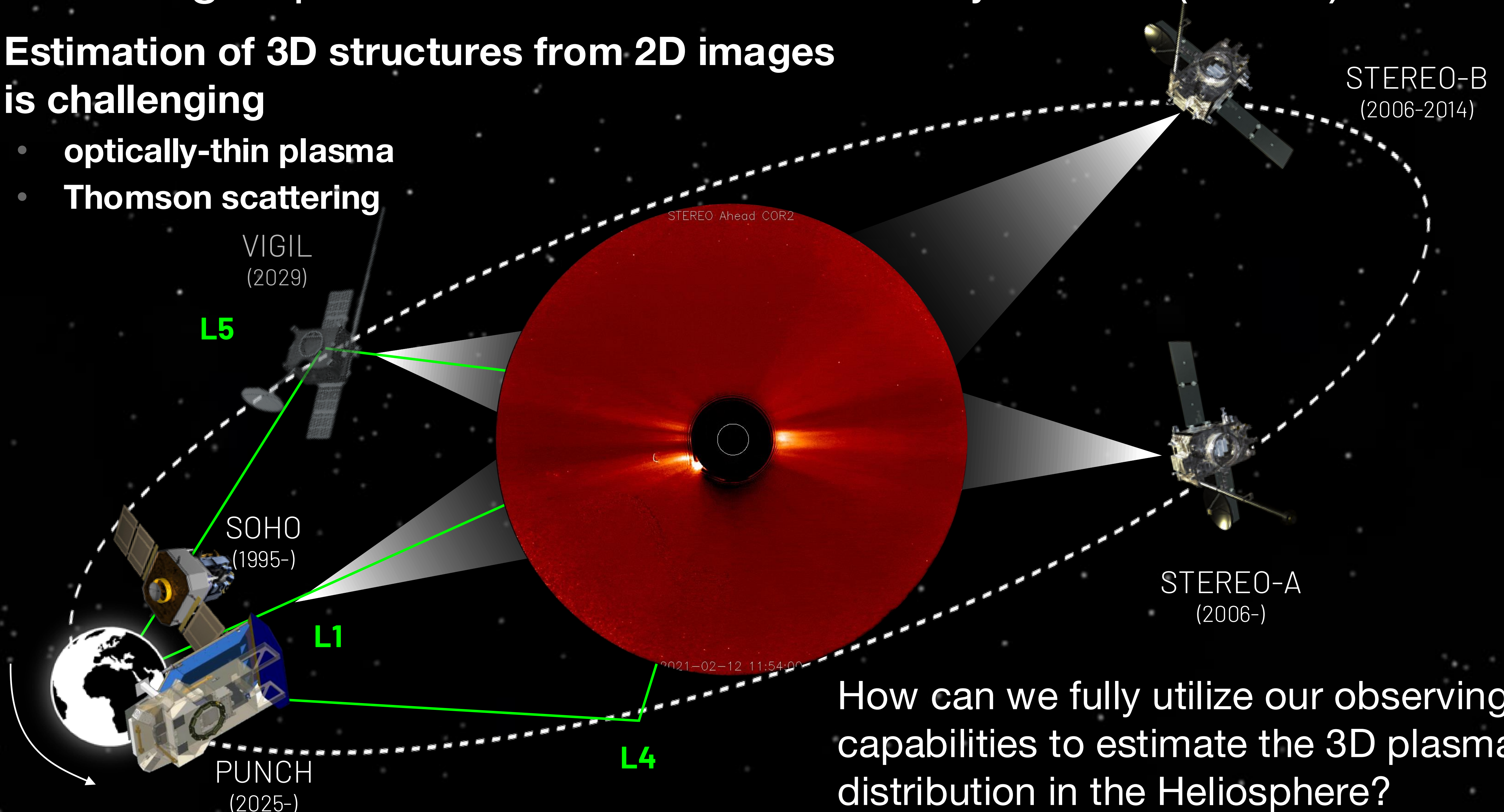

How can we fully utilize our observing capabilities to estimate the 3D plasma distribution in the Heliosphere?

Tomographic reconstruction with Physics-Informed Neural Radiance Fields

- Based on Neural Radiance Fields (Mildenhall et al. 2021) → **SuNeRF** **(Jarolim et al. 2023)**

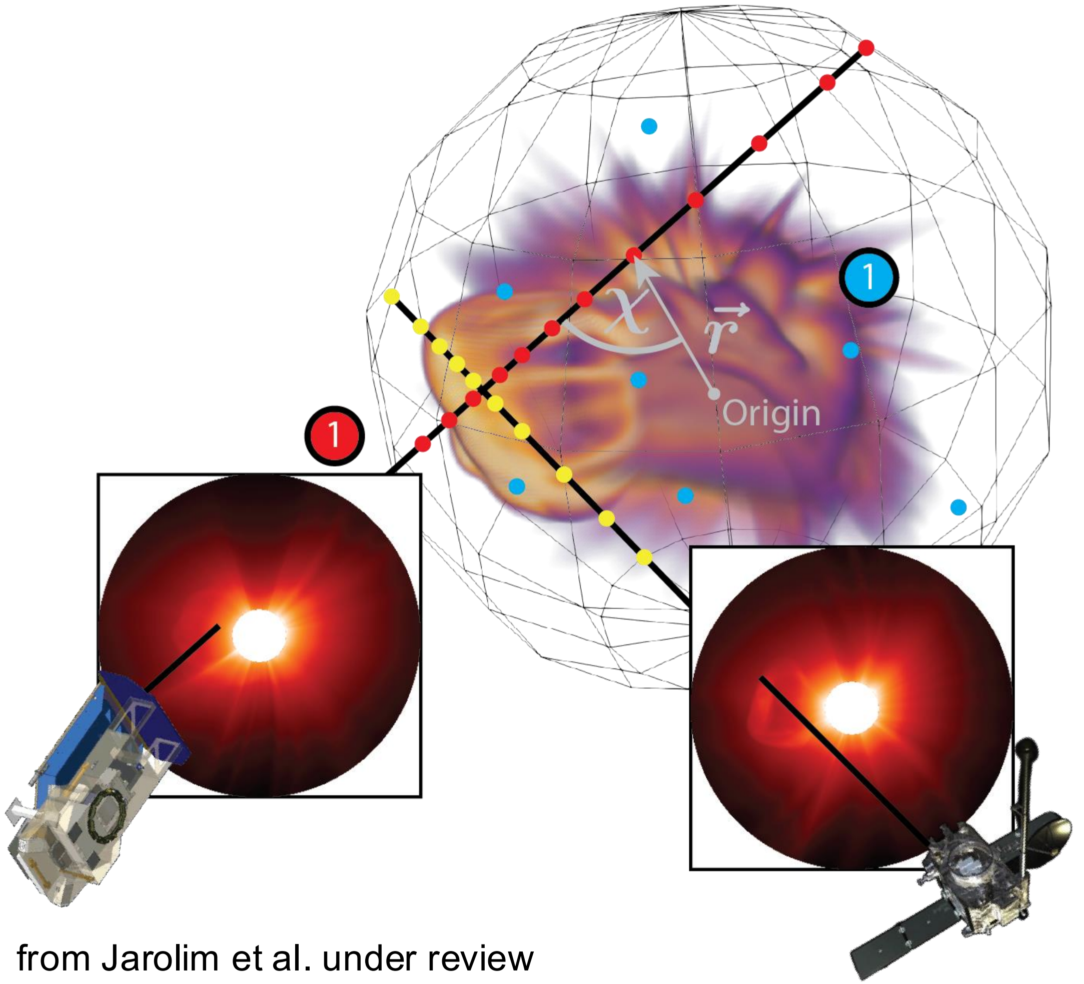

from Jarolim et al. under review

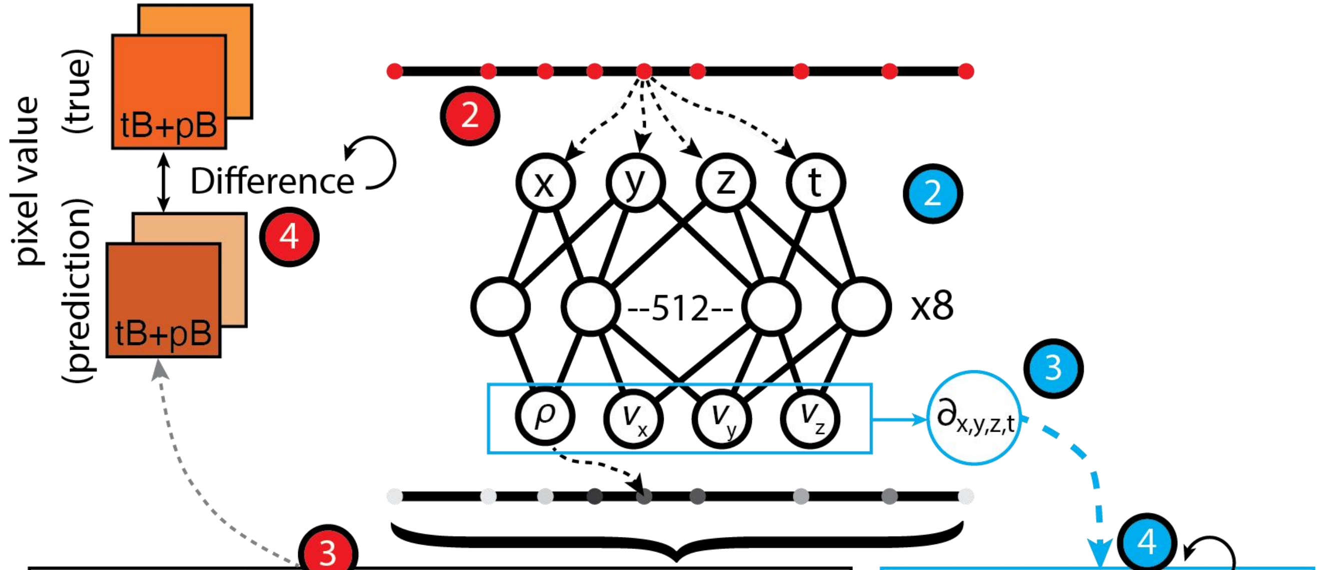

$$tB = C \int \rho(\vec{r}) \left[f_T(\vec{r}) - \sin^2(\chi) f_P(\vec{r}) \right] dl$$

$$pB = C \int \rho(\vec{r}) \left[\sin^2(\chi) f_P(\vec{r}) \right] dl$$

$$\frac{\partial \rho}{\partial t} + \nabla \cdot (\rho \vec{v}) = 0$$

$$\frac{\|\vec{v} \times \vec{r}\|}{\|\vec{v}\| \, \|\vec{r}\|} = 0$$

$$(\|\vec{v}\| - v_{\min})^2 \text{ if } \|\vec{v}\| < v_{\min}$$
$$(\|\vec{v}\| - v_{\max})^2 \text{ if } \|\vec{v}\| > v_{\max}$$

CME Dataset

- Validation with **synthetic PUNCH observations** (Credits: A. Malanushenko)
  - GAMERA simulation – **0.1 AU to 100 $R_\odot$**
  - Ground truth reference – **electron density**
  - Idealized (no noise, artifacts, background stars)
  - Different **observer configurations** used for **method validation**

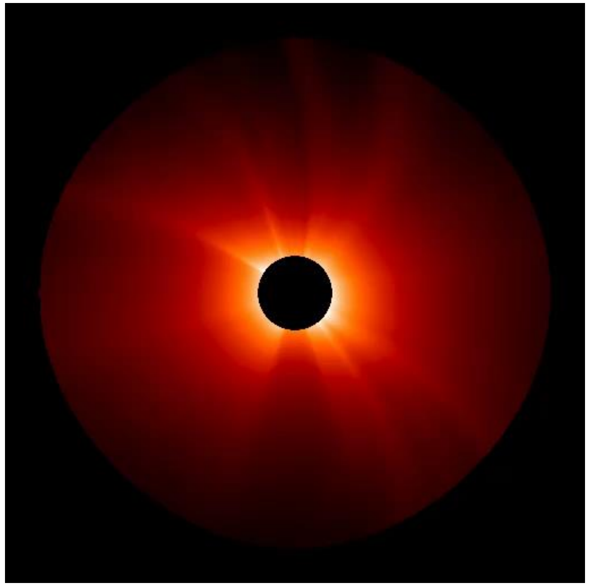

Polarized Brightness – Obs. 1

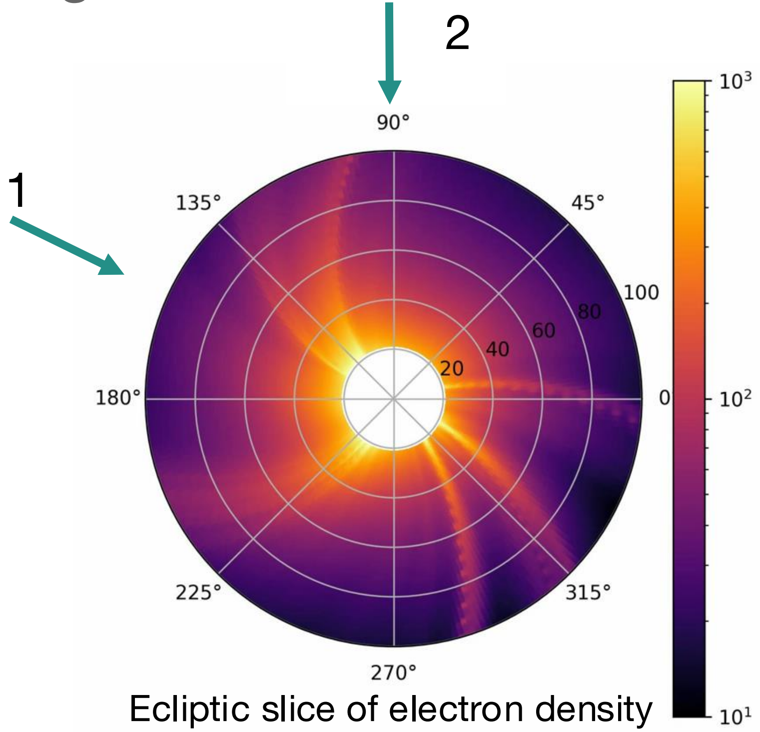

Ecliptic slice of electron density

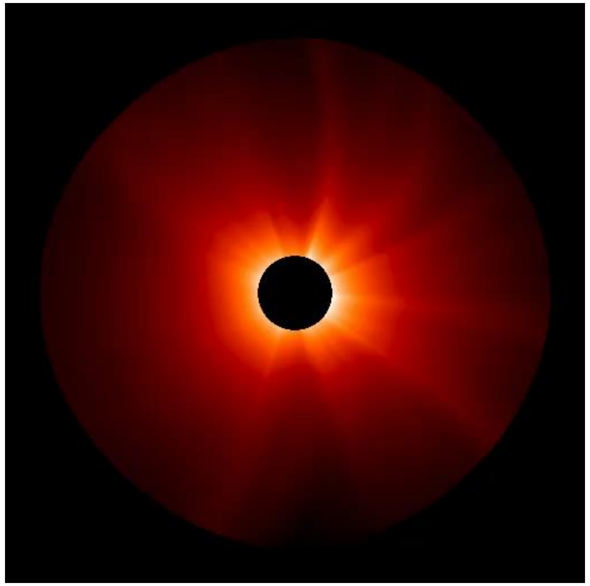

Polarized Brightness – Obs. 2

3D reconstruction of CMEs

- Comparison of **latitudinal** and **longitudinal slices**
- Different observer configurations → **blue arrows**
- More viewpoints lead to better reconstructions
- **2 viewpoints** can provide a **full 3D reconstruction** of the CME

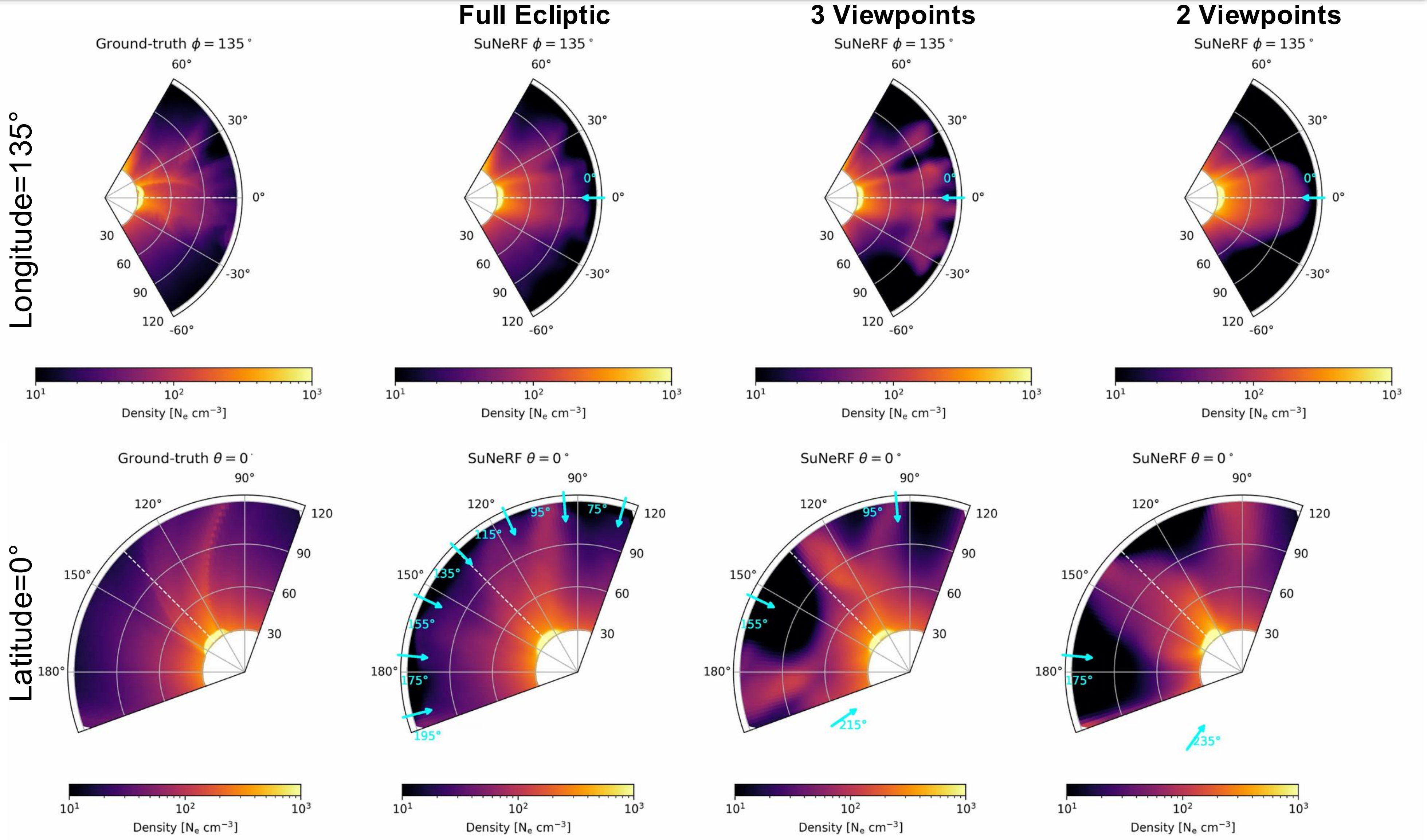

CME Tomography – 2 Viewpoints

- Tomographic reconstruction
  - **Bright front** (high-density) + variations
  - **Dark cavity** (low-density)
  - **Bright core** (high-density)
- **2 Viewpoints** are sufficient to resolve the **3D topology of CMEs**
- Correct reconstruction of **deformed front**

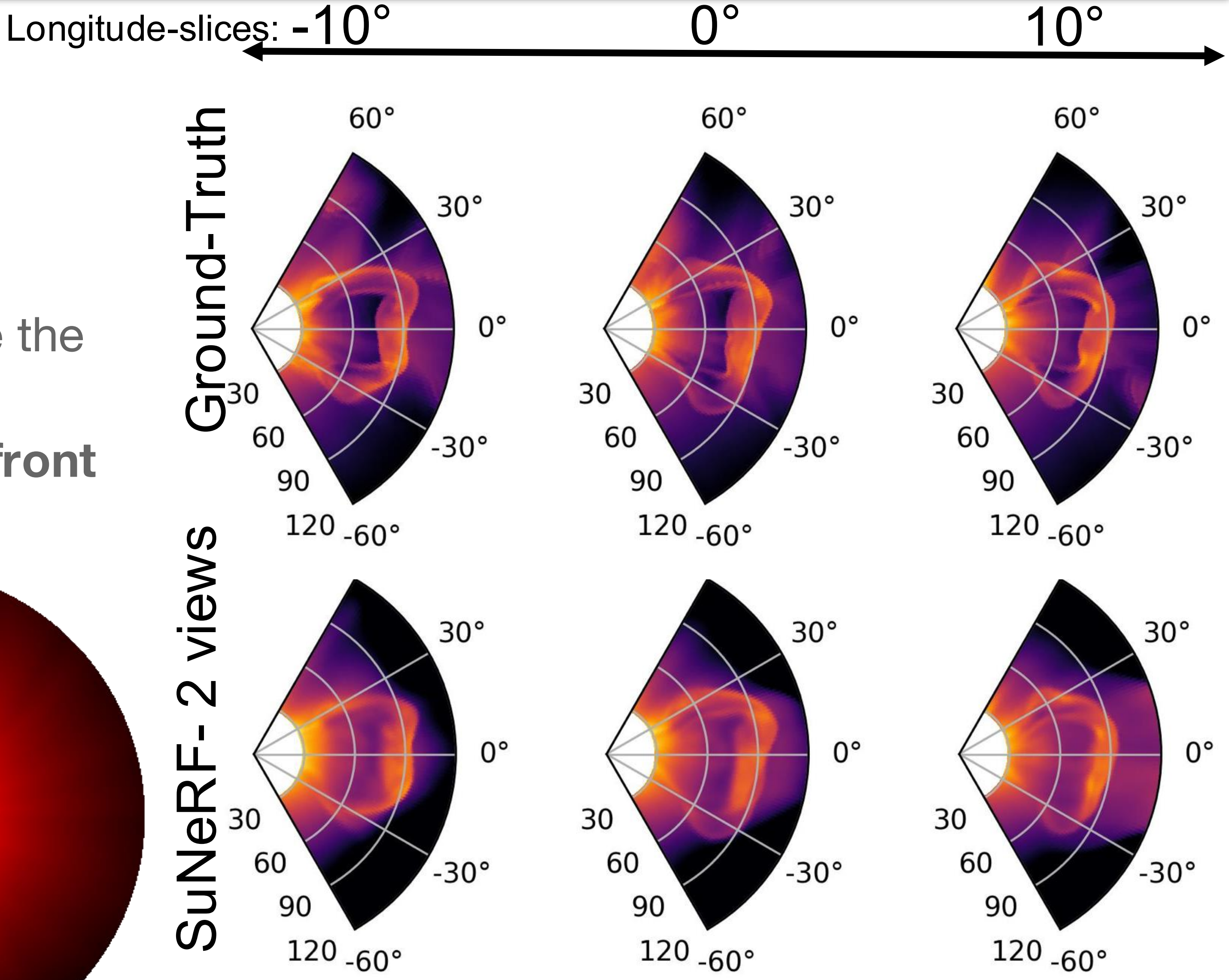

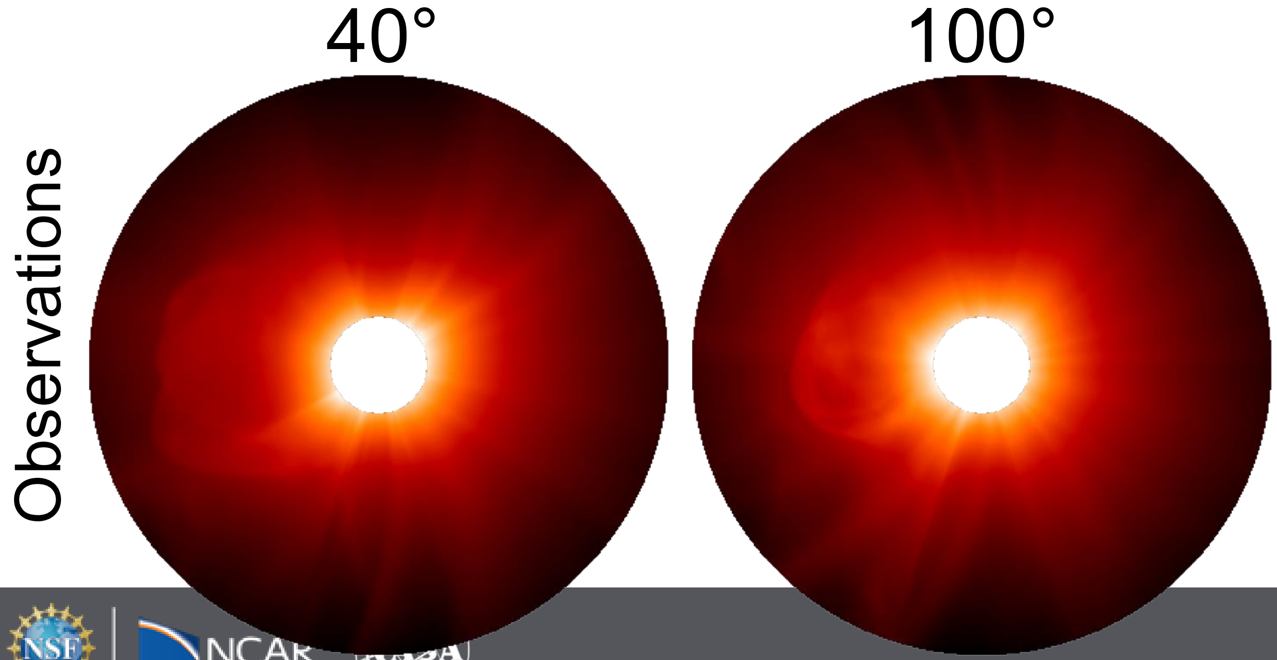

CME Tomography – 2 Viewpoints

- Tomographic reconstruction
  - **Bright front** (high-density) + variations
  - **Dark cavity** (low-density)
  - **Bright core** (high-density)
- **2 Viewpoints** are sufficient to resolve the **3D topology of CMEs**
- Correct reconstruction of **deformed front**

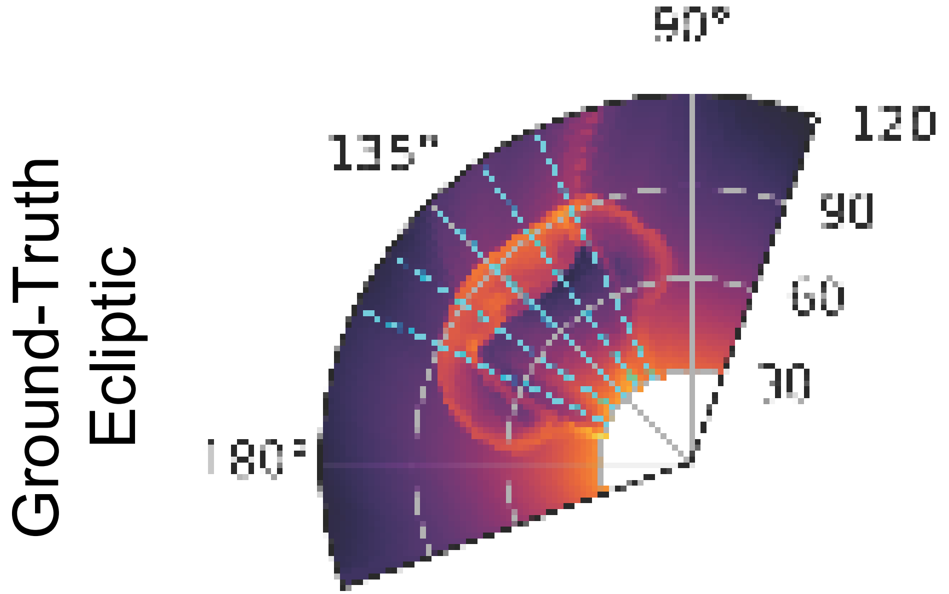

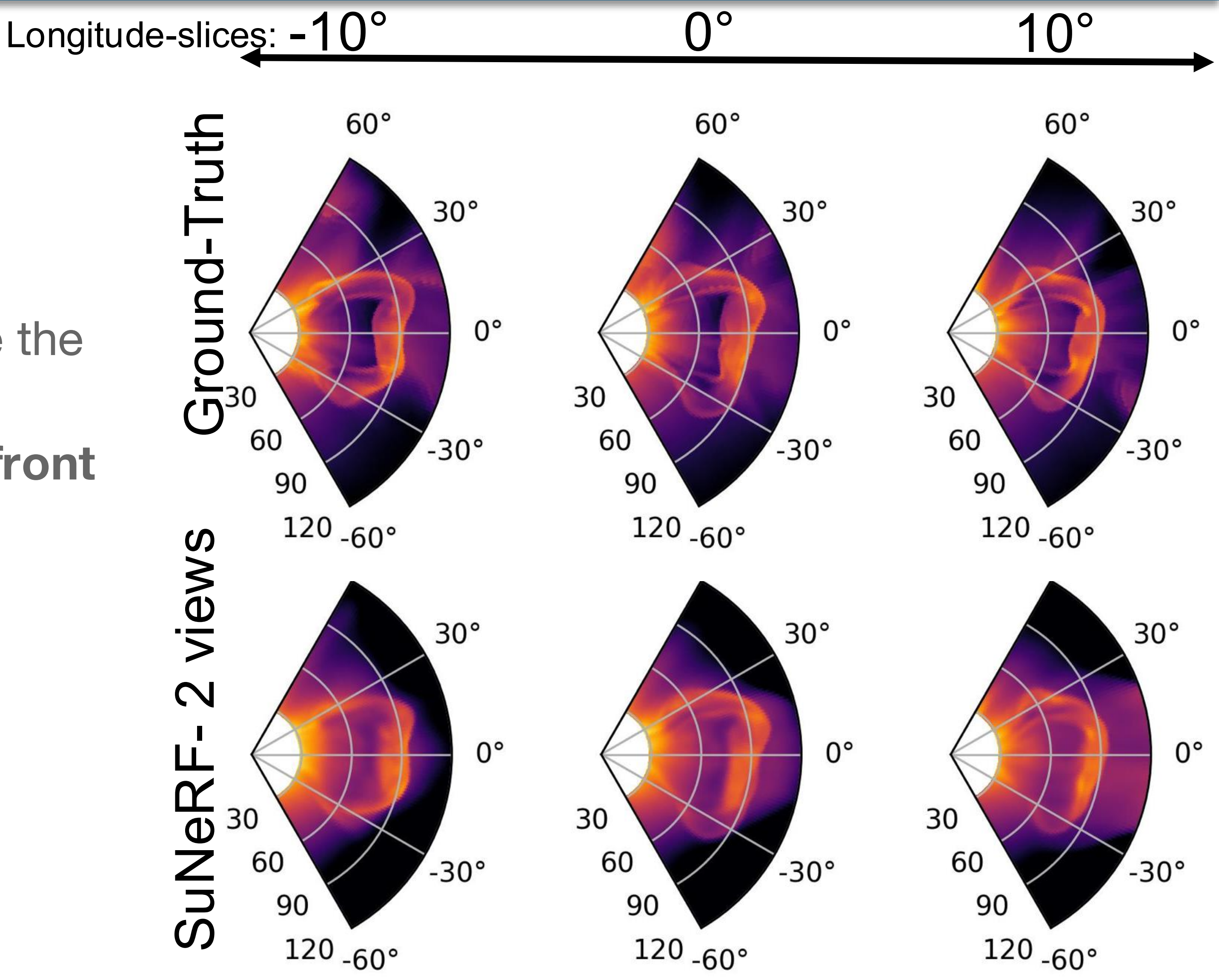

Full CME Tomography – 2 Viewpoints

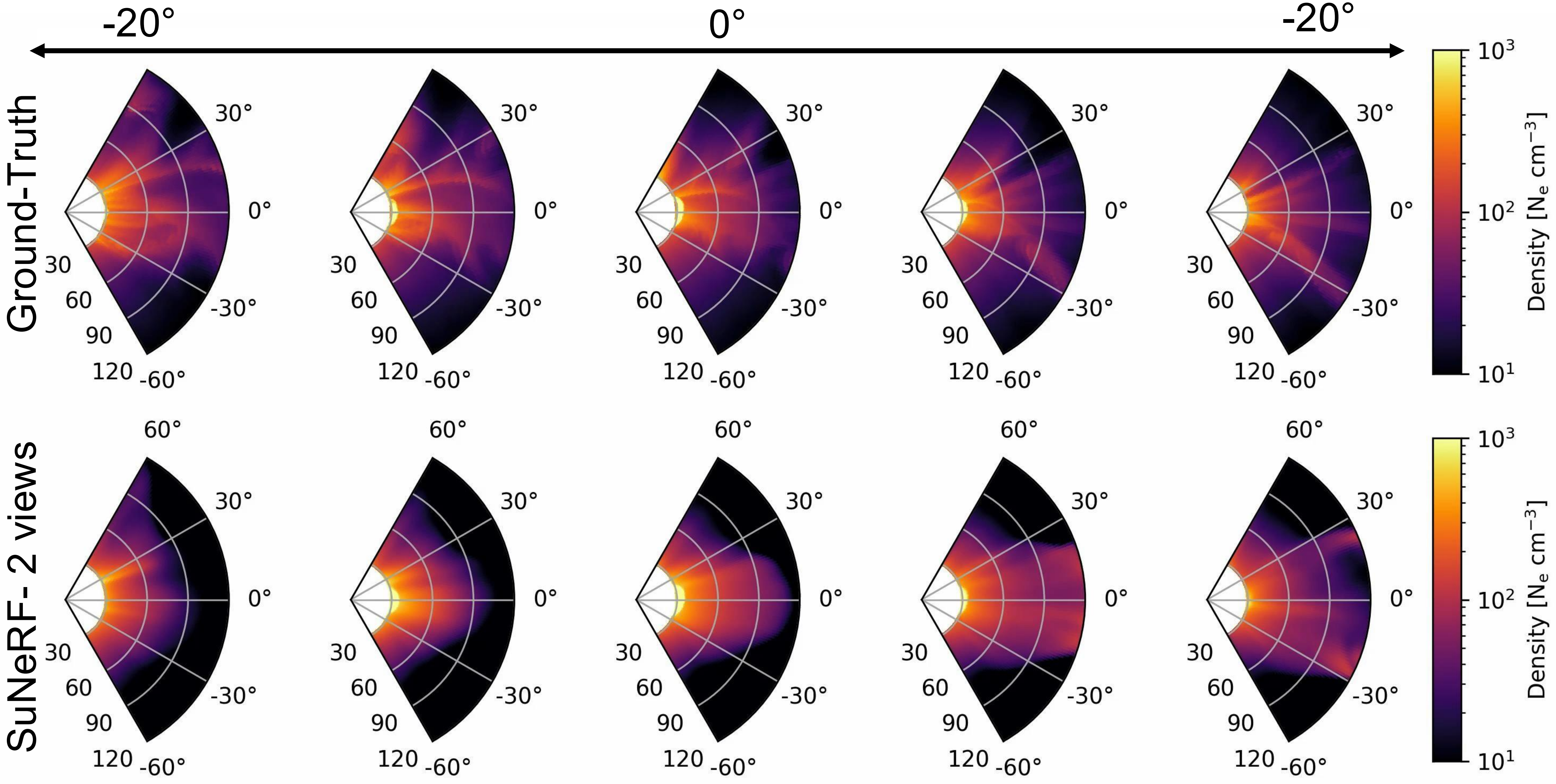

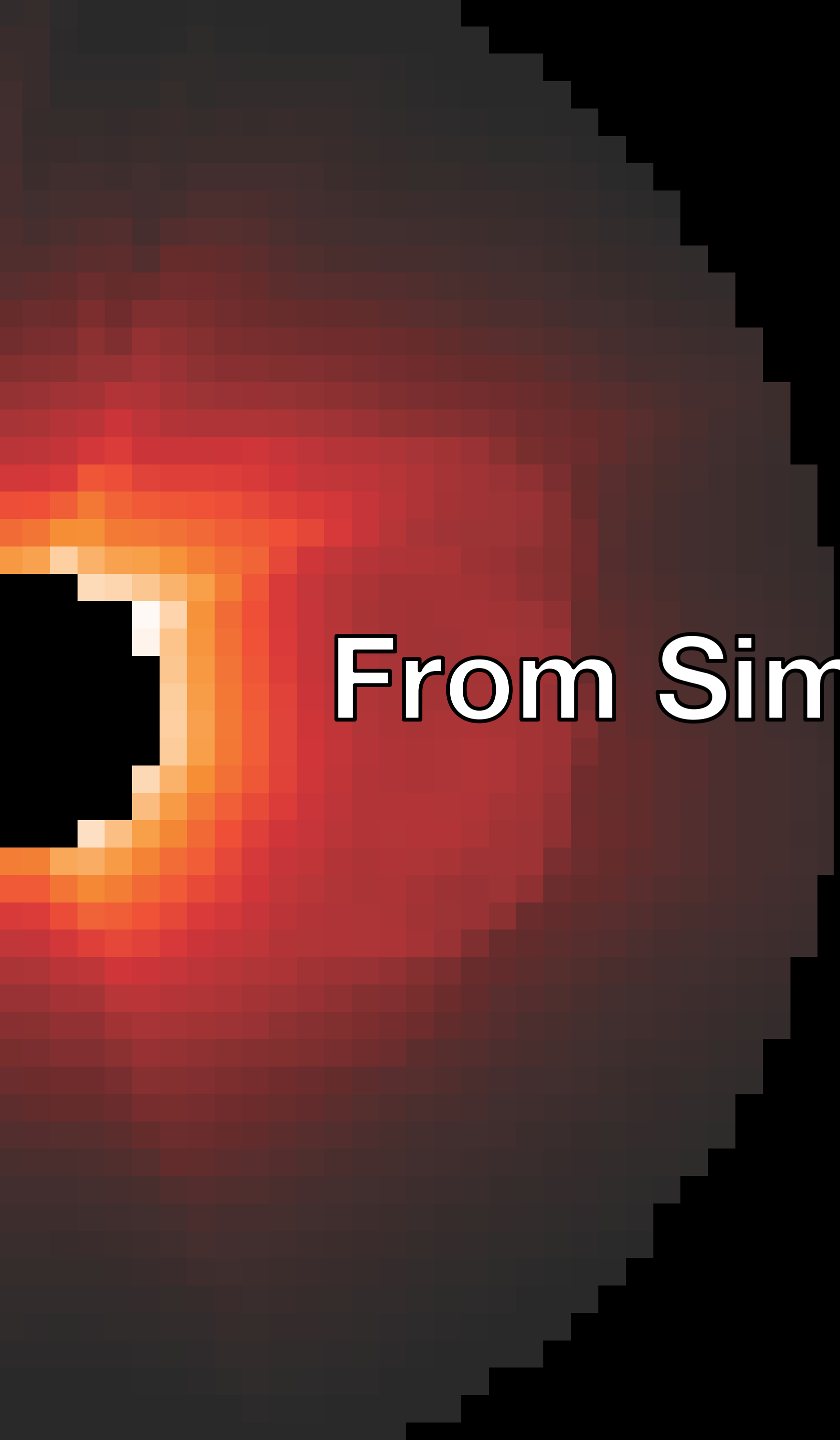

From Simulations to Observations

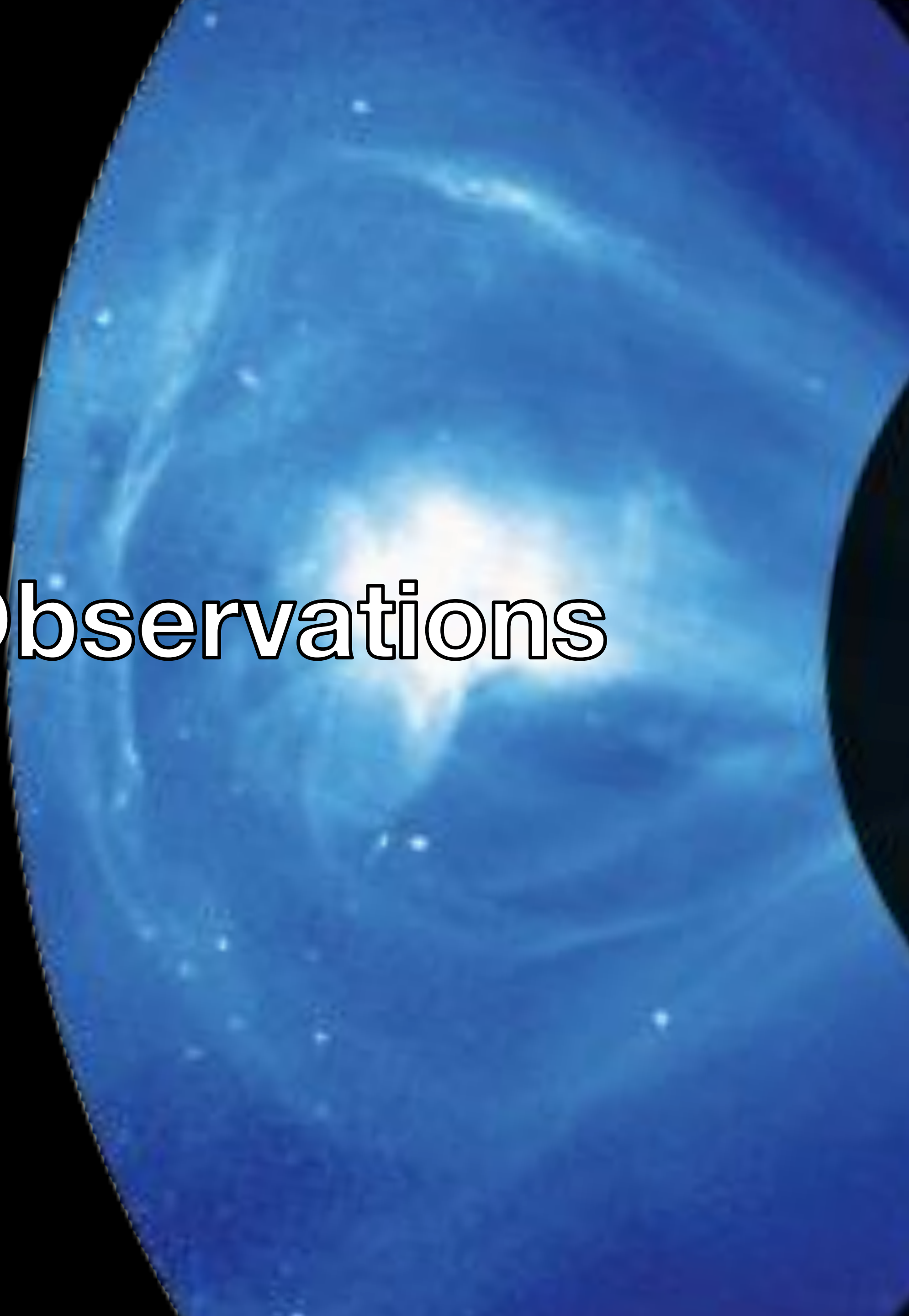

Learned Corrections

- Observational data has artifacts, calibration issues, and F-corona contributions
- We include additional **learnable correction masks →** separate noise and data as part of the reconstruction

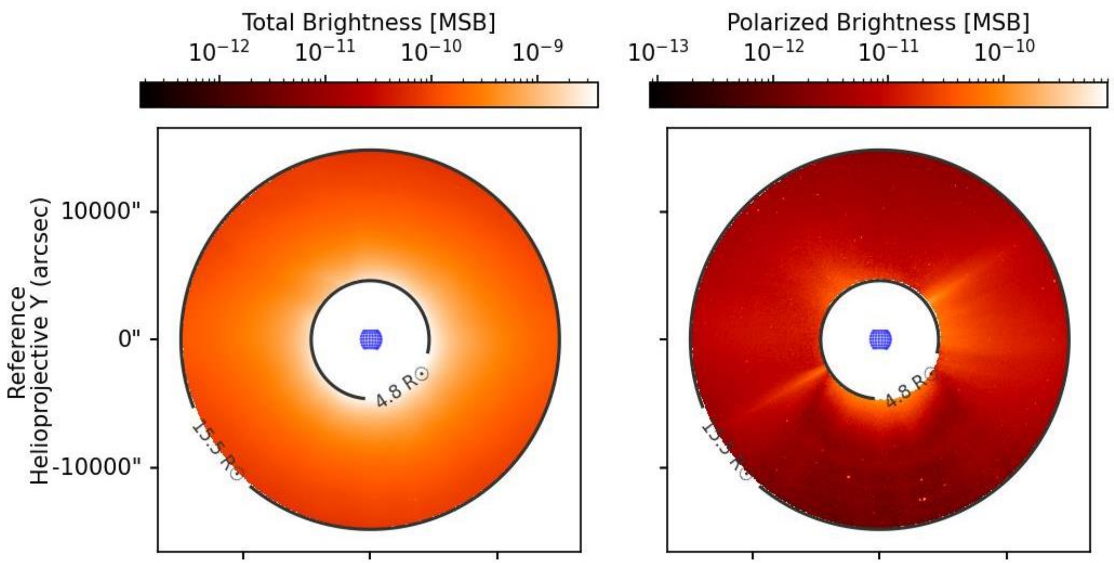

Learned Corrections

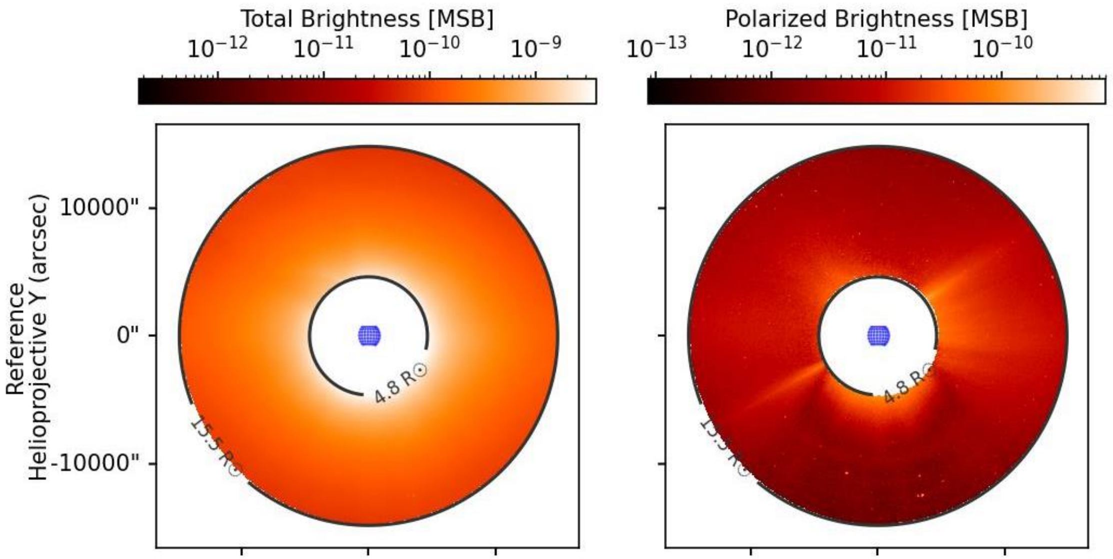

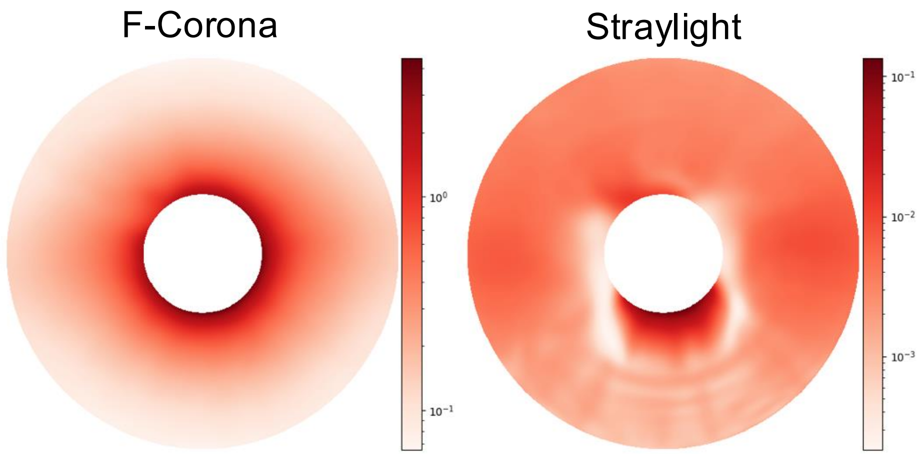

Learned Corrections

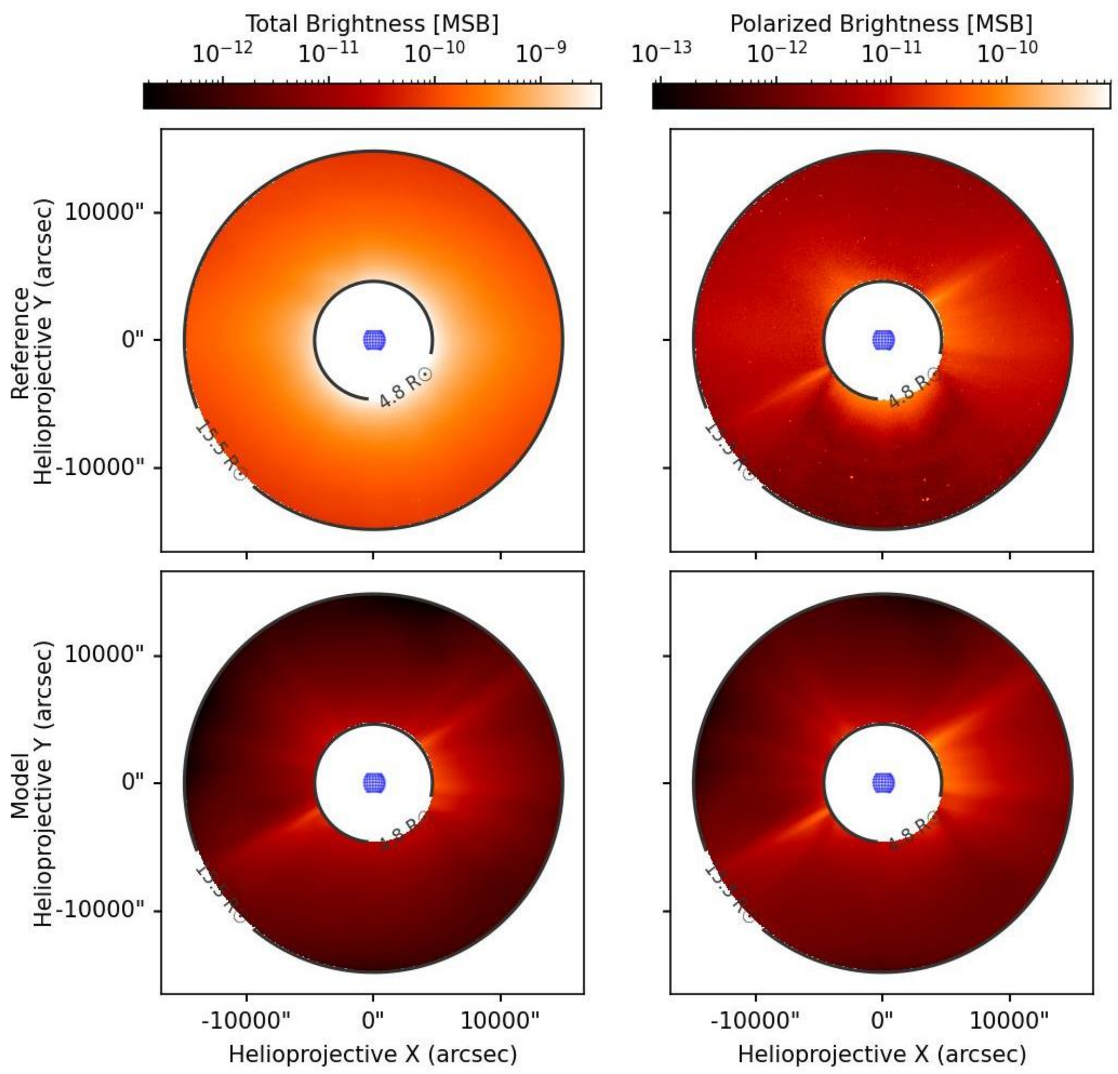

−

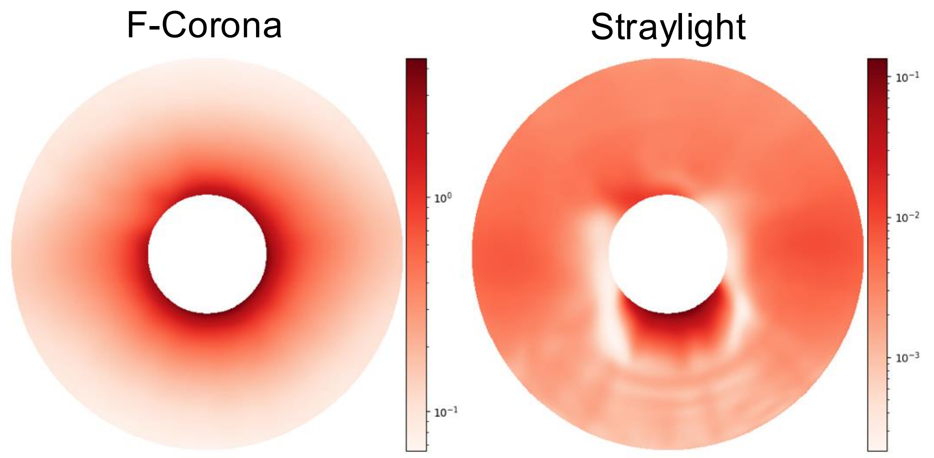

PUNCH corrections

- **Observational gaps** interpolated through temporal smoothness + physics constraints
- Continuity equation enforces physical **stratification of solar atmosphere**
- Over- and Under-subtraction are intrinsically corrected

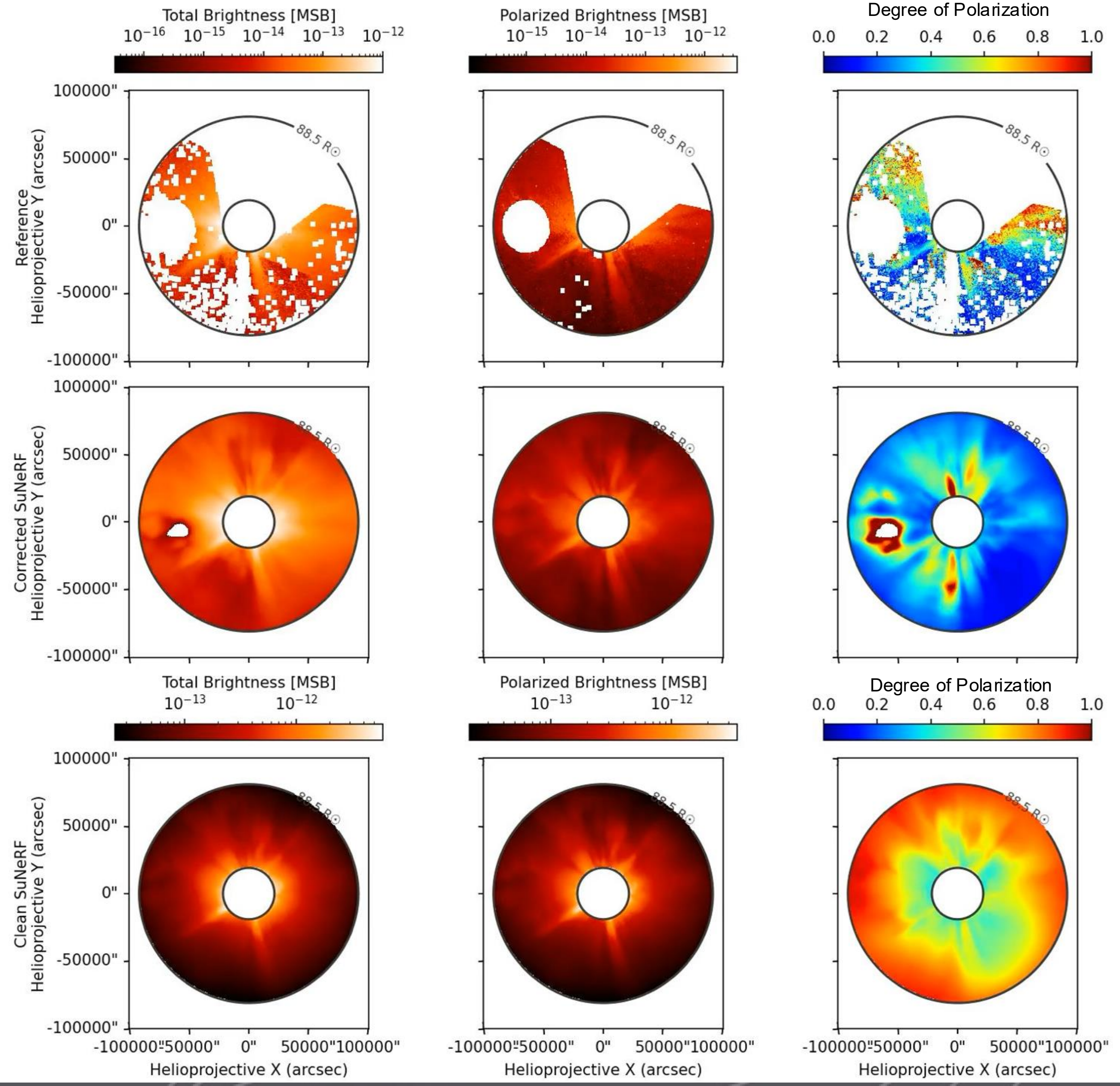

NSF NCAR NASA

Application to Observations

- Reconstruction based on: **PUNCH/WFI, STREREO-A/COR2, GOES/CCOR**
- Video: observer location, forward rendered pB from 3D reconstruction, integrated density
- Combined view from **3 to 50** $R_\odot$

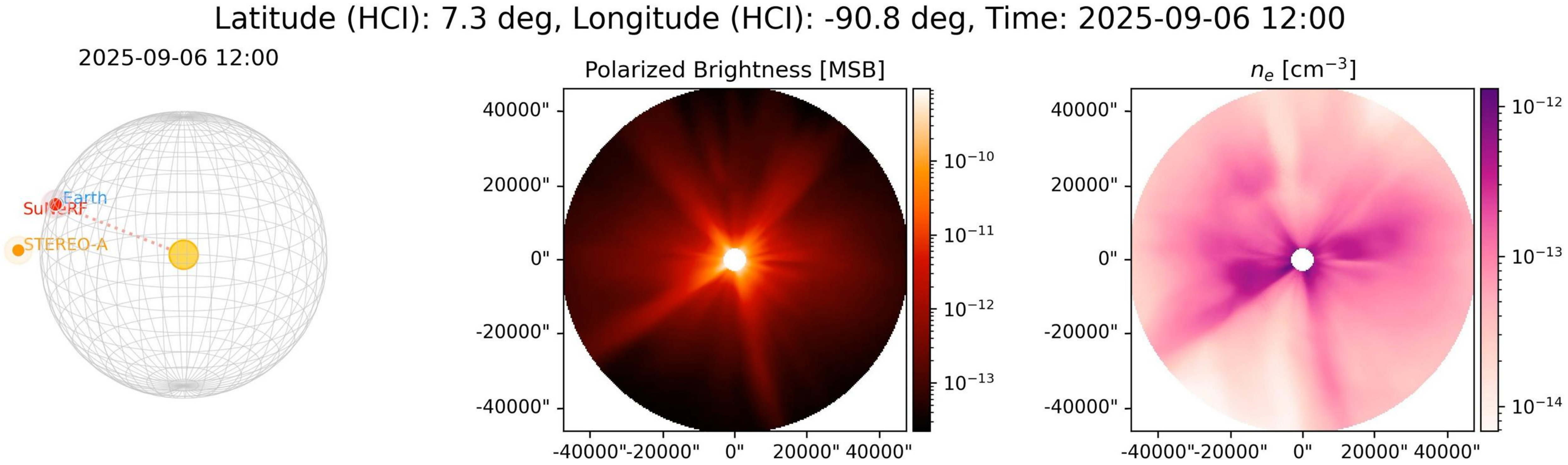

Coronal Mass Ejection from April 2026

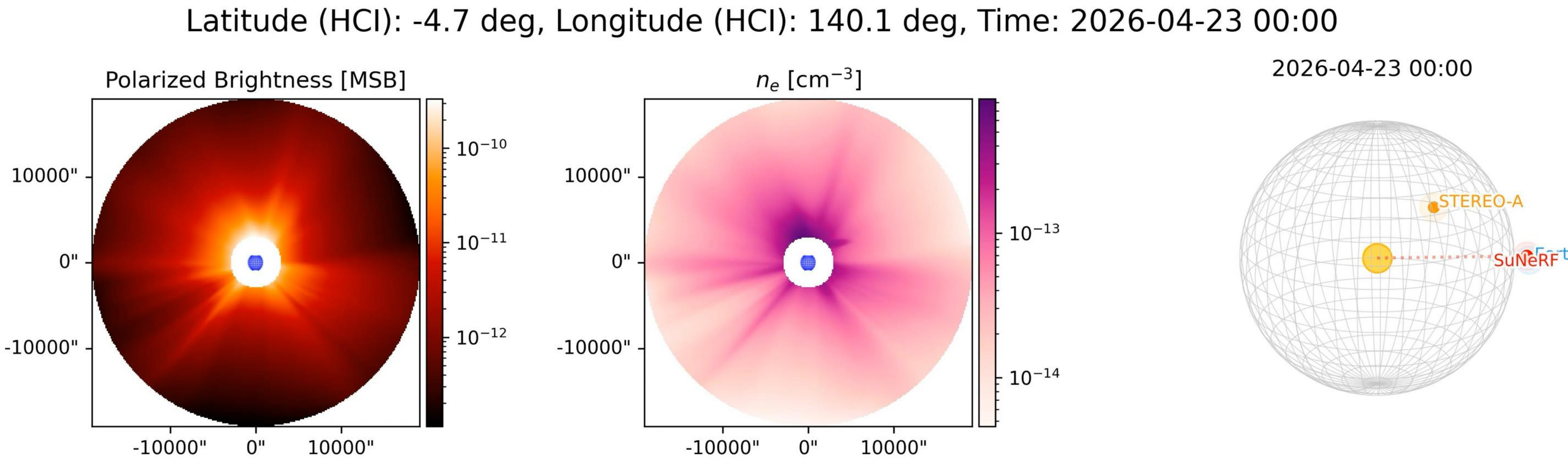

Coronal Mass Ejection from April 2026

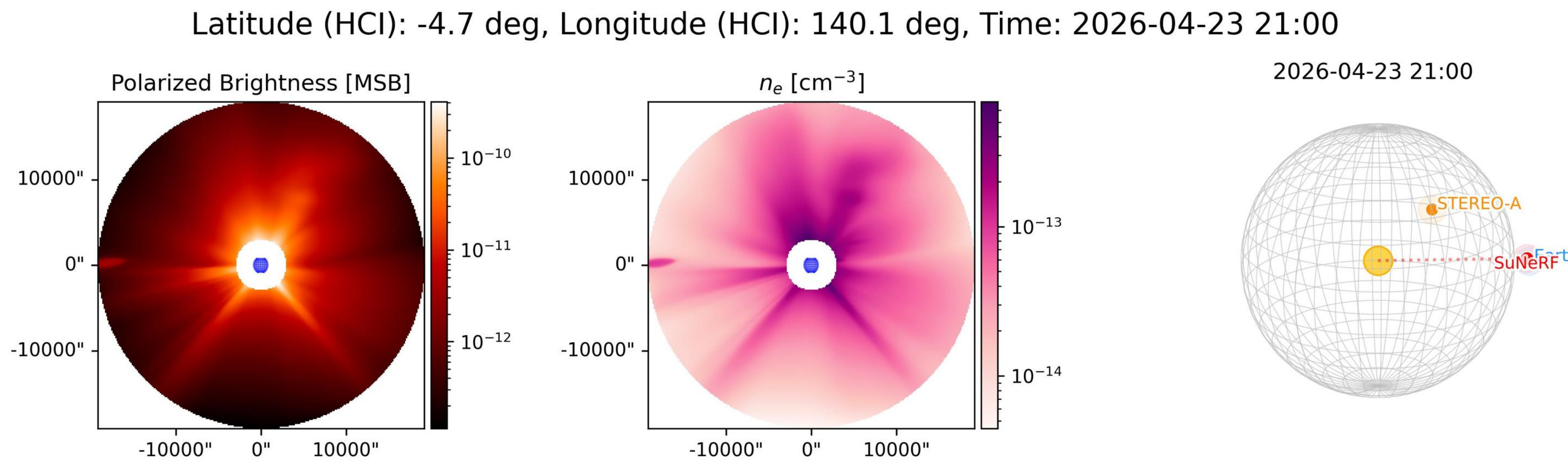

Coronal Mass Ejection from April 2026

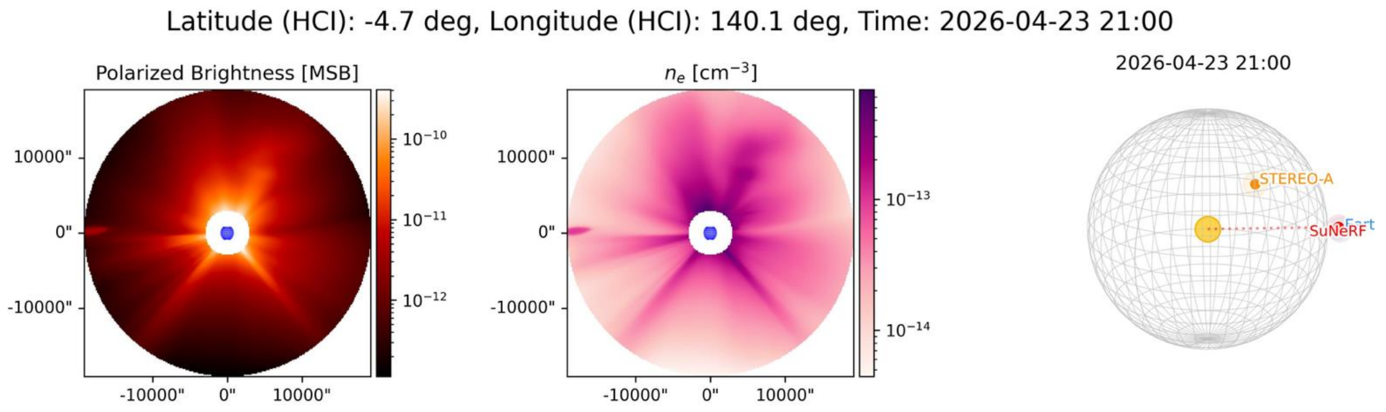

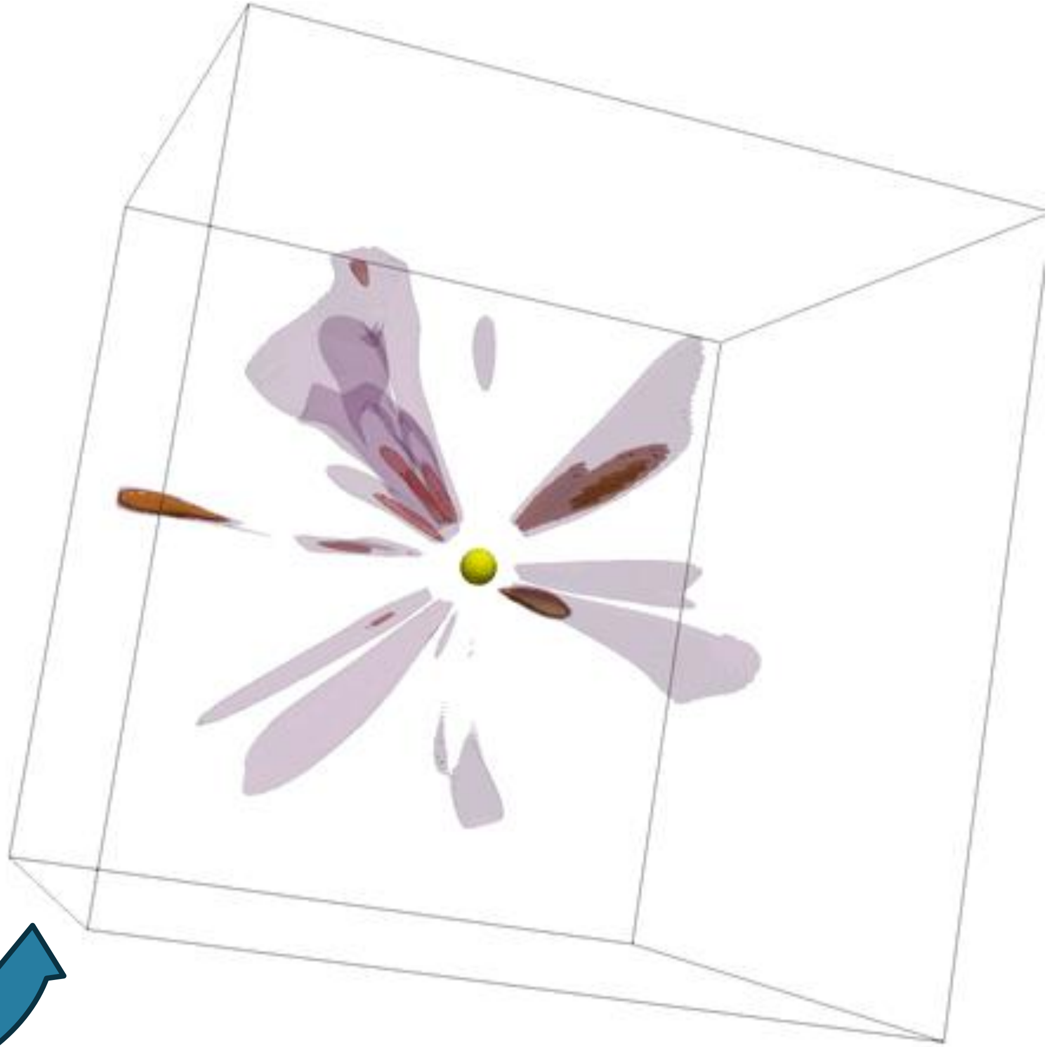

Probing the 3D morphology of CMEs

- Reconstruction based on: **STREREO-A/COR2, STREREO-B/COR2 (2010-03)**
- Video: slices at constant longitude of **electron density** (top) and **velocity** (bottom)

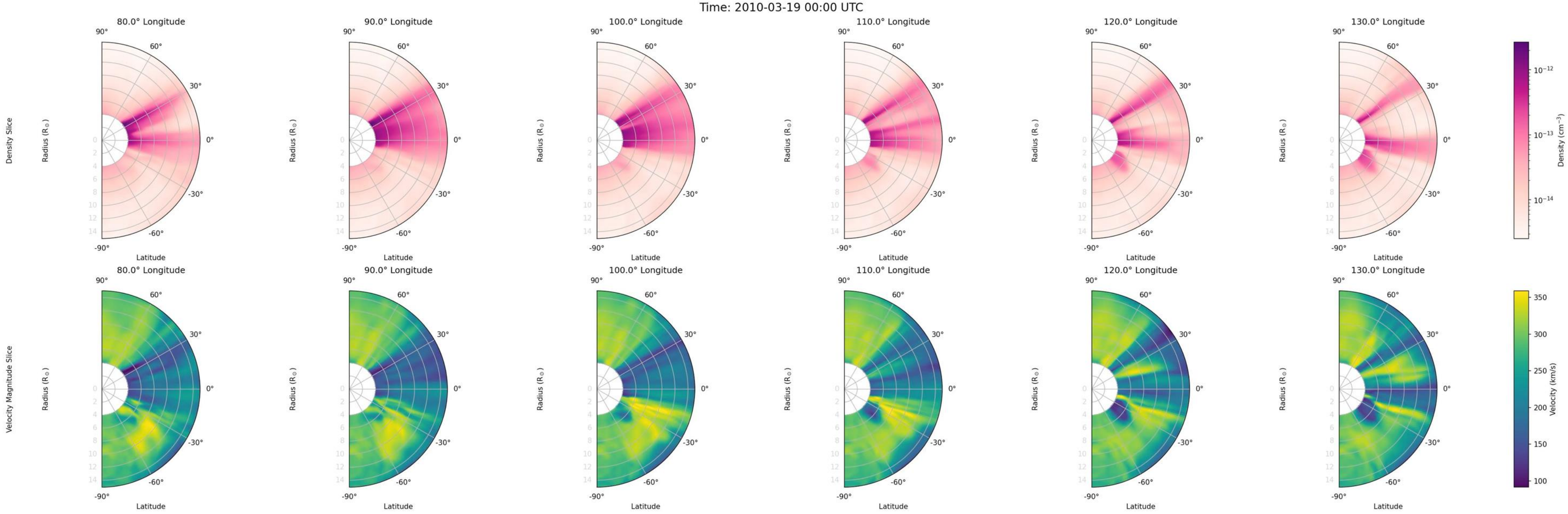

Inferred 3D Velocity Field

- **Density** and **Velocity** at radial slices
  - **5 to 15** $R_\odot$
  - Velocities through **continuity equation**
- **Coronal holes** → fast solar wind
  - Low density
  - High velocities
- **Streamers** → slow solar wind
  - High density
  - Low velocities
- Visible CME shocks in the corona

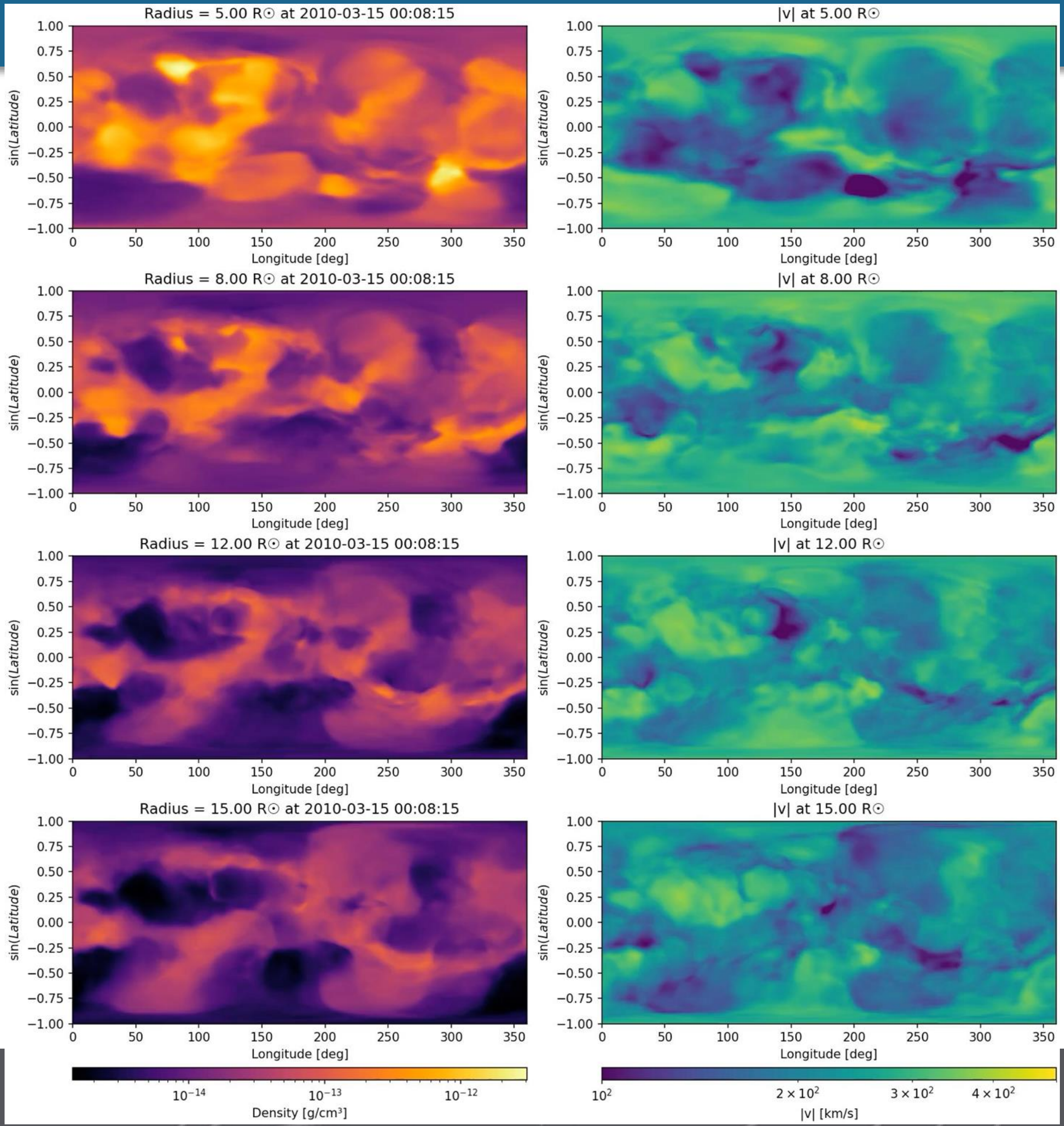

Conclusion

- Physics-Informed Neural Radiance Fields enable 3D reconstruction of the Heliosphere from sparse observations
  - Including physical constraints can overcome viewpoint limitations
  - Combines multiple observations into a physically consistent 3D representation of the Heliosphere
- **Next steps**:
  - Integrated EUV + white-light tomography
  - Advance physics model
  - Additional instruments (HI, in-situ)
- **SuNeRF:** github.com/RobertJaro/SuNeRF
  - **Jarolim et al. 2024**
    ApJL 961 L31
- **SuNeRF-CME**;
  - **Jarolim et al. under review**

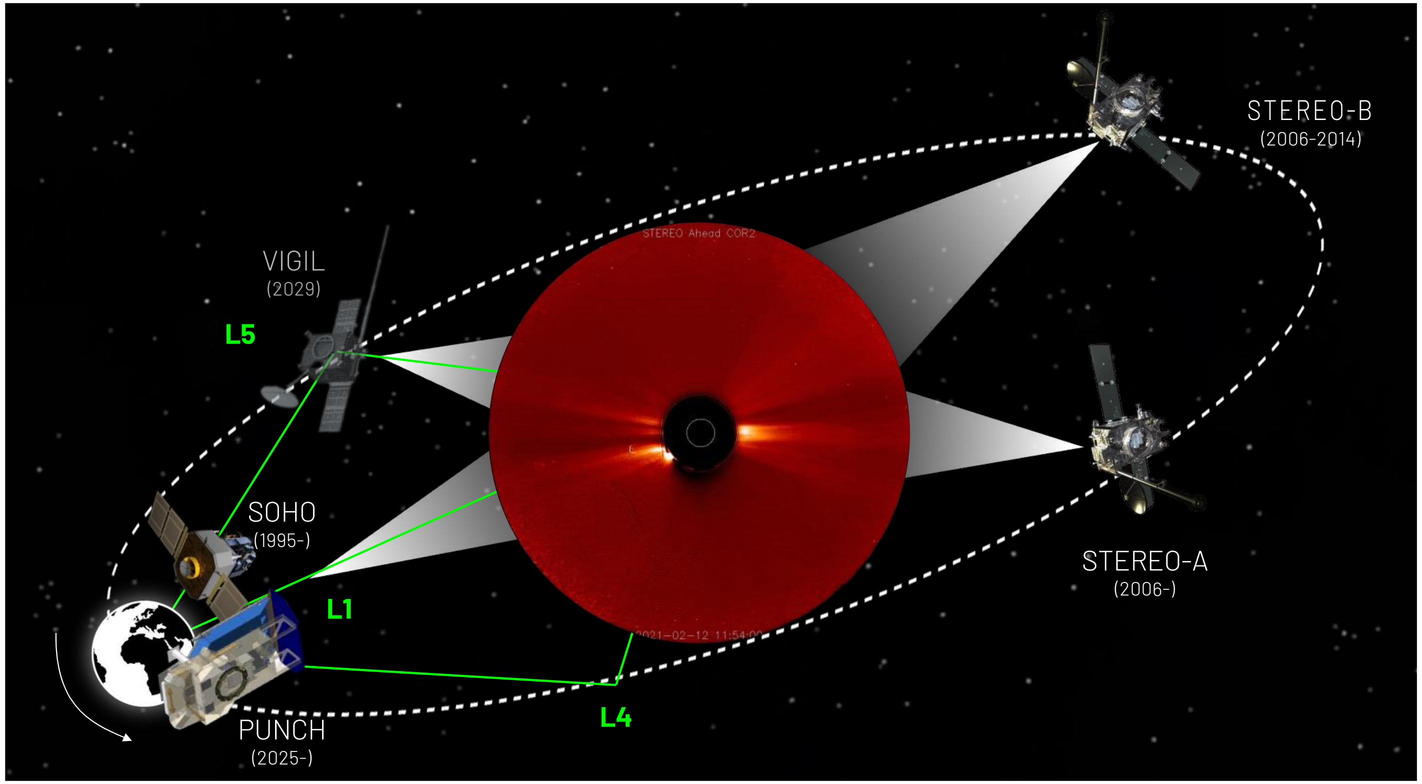

Thank you!

Robert Jarolim
NASA Jack Eddy Fellow
High Altitude Observatory, NSF NCAR

This material is based upon work supported by the National Center for Atmospheric Research, which is a major facility sponsored by the National Science Foundation under Cooperative Agreement No. 1852977.

References

- Raissi, M., et al. Physics-informed neural networks: A deep learning framework for solving forward and inverse problems involving nonlinear partial differential equations.Journal of Computational Physics 378, 686–707 (2019).
- Karniadakis, George Em, et al. "Physics-informed machine learning." Nature Reviews Physics 3.6 (2021): 422-440.
- Jarolim, R., et al. "Probing the solar coronal magnetic field with physics-informed neural networks." Nature Astronomy 7.10 (2023): 1171-1179.
- Jarolim, R., et al. "Advancing Solar Magnetic Field Extrapolations through Multiheight Magnetic Field Measurements." The Astrophysical Journal Letters 963.1 (2024): L21.
- Wiegelmann, T., et al. Coronal Magnetic Field Models. 210, 249–274 (2017).
- Baty, Hubert, and Vincent Vigon. "Modelling solar coronal magnetic fields with physics-informed neural networks." Monthly Notices of the Royal Astronomical Society 527.2 (2024): 2575-2584.
- Camporeale, Enrico, et al. "Data-driven discovery of Fokker-Planck equation for the Earth's radiation belts electrons using Physics-Informed neural networks." Journal of Geophysical Research: Space Physics 127.7 (2022): e2022JA030377.
- Baso, C. J., et al. "Exploring spectropolarimetric inversions using neural fields. Solar chromospheric magnetic field under the weak-field approximation." arXiv preprint arXiv:2409.05156 (2024).
- Athalathil, Jithu J., et al. "Surface Flux Transport Modeling Using Physics-informed Neural Networks." The Astrophysical Journal 975.2 (2024): 258.
- Bintsi, Kyriaki-Margarita, et al. "SuNeRF: Validation of a 3D Global Reconstruction of the Solar Corona Using Simulated EUV Images." arXiv preprint arXiv:2211.14879 (2022).
- Jarolim, Robert, et al. "SuNeRF: 3D reconstruction of the solar EUV corona using Neural Radiance Fields." The Astrophysical Journal Letters 961.2 (2024): L31.

Backup Slides

Application to Filament Eruption (Jarolim et al. 2024)

- White-light and EUV observations could be combined into a single 3D reconstruction
- 3D reconstruction of filament eruption
- Reconstruction from 2 viewpoints (SDO/AIA + STEREO-A/EUVI)

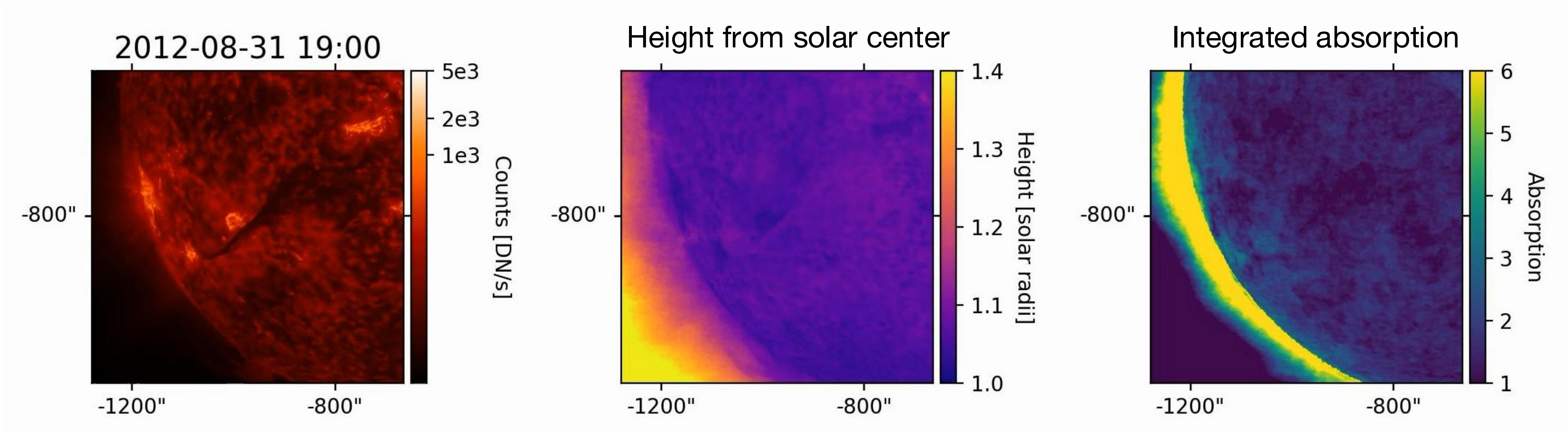

Outlook: Density and Temperature reconstructions

- Tomographic reconstruction of **electron density and temperature** through the **temperature response function**
- Directly combines observations of SDO/AIA and Solar Orbiter/EUI
- 3D density reconstruction of Coronal Hole Boundaries, Active Regions, and Filaments
- a) emission measure; b) rendered SDO/AIA filtergram; c) slice through 3D atmosphere

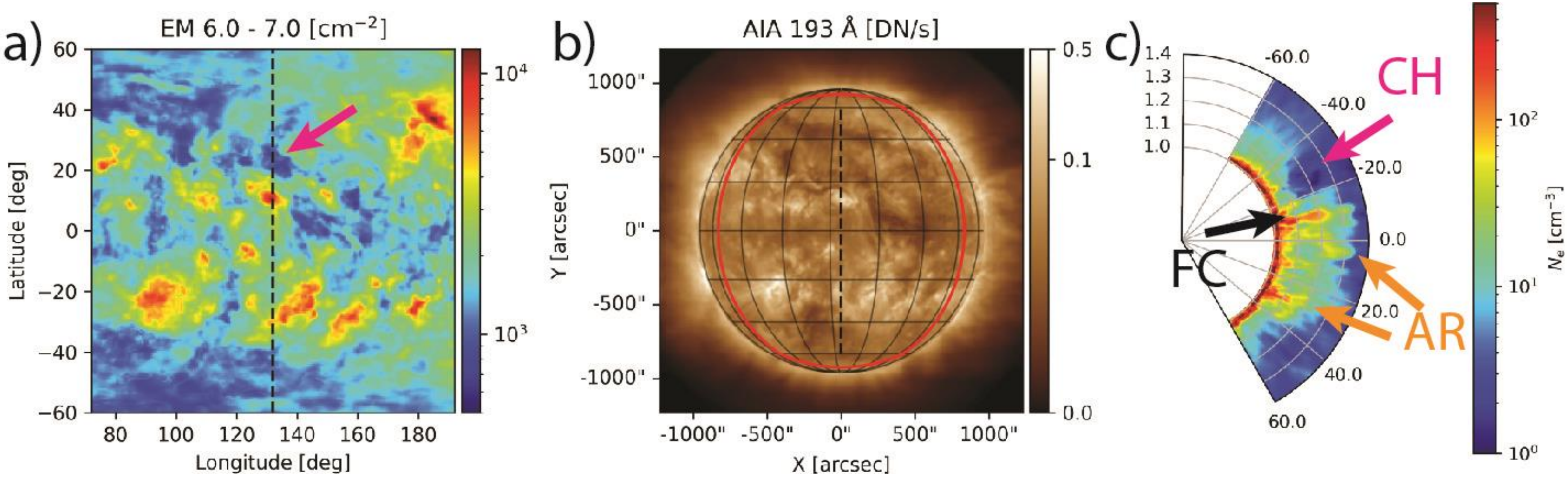

Jarolim et al. in prep, results in model units

Stress Test – Rendered Polar View

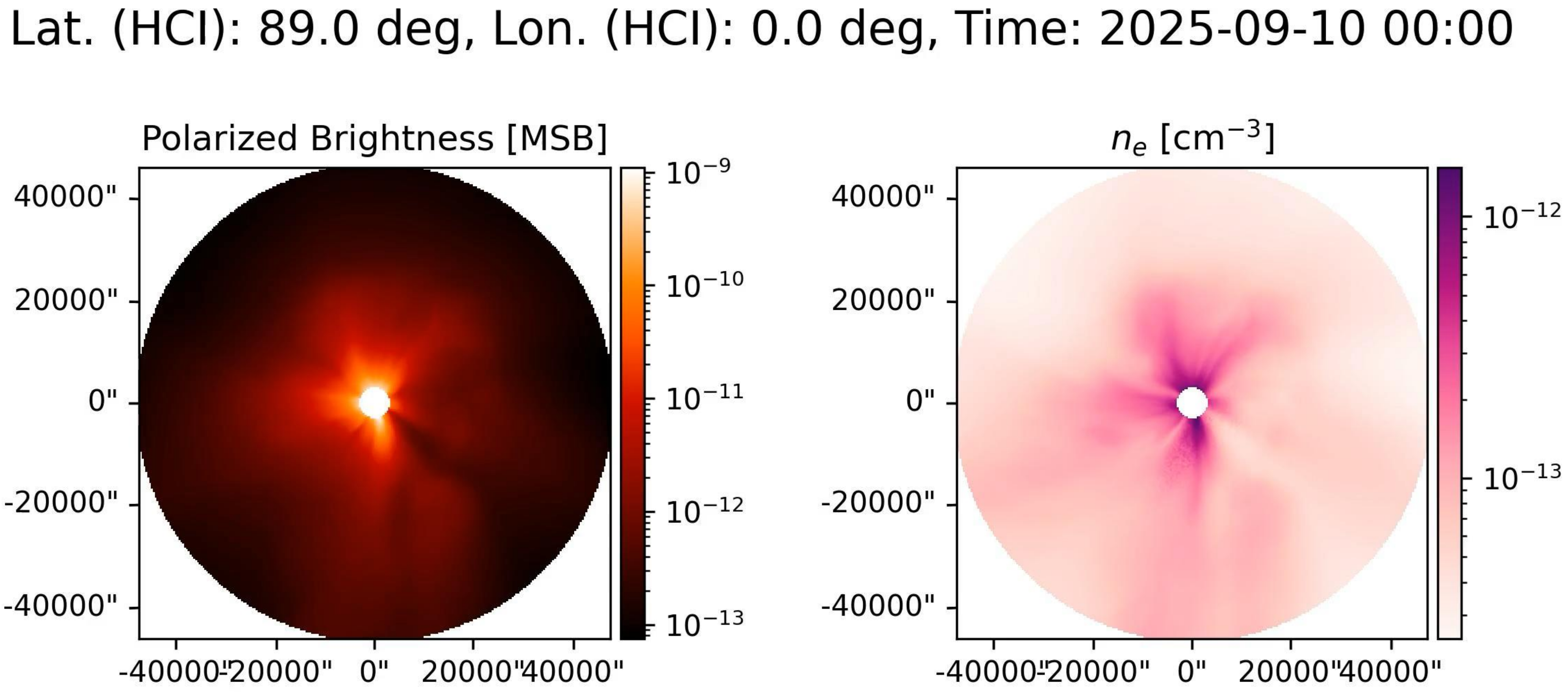

Application to Observations - PUNCH

- Reconstruction based on: **PUNCH/WFI, STREREO-A/COR2, GOES/CCOR**
- Video: forward rendered pB from 3D reconstruction, integrated density, observer location

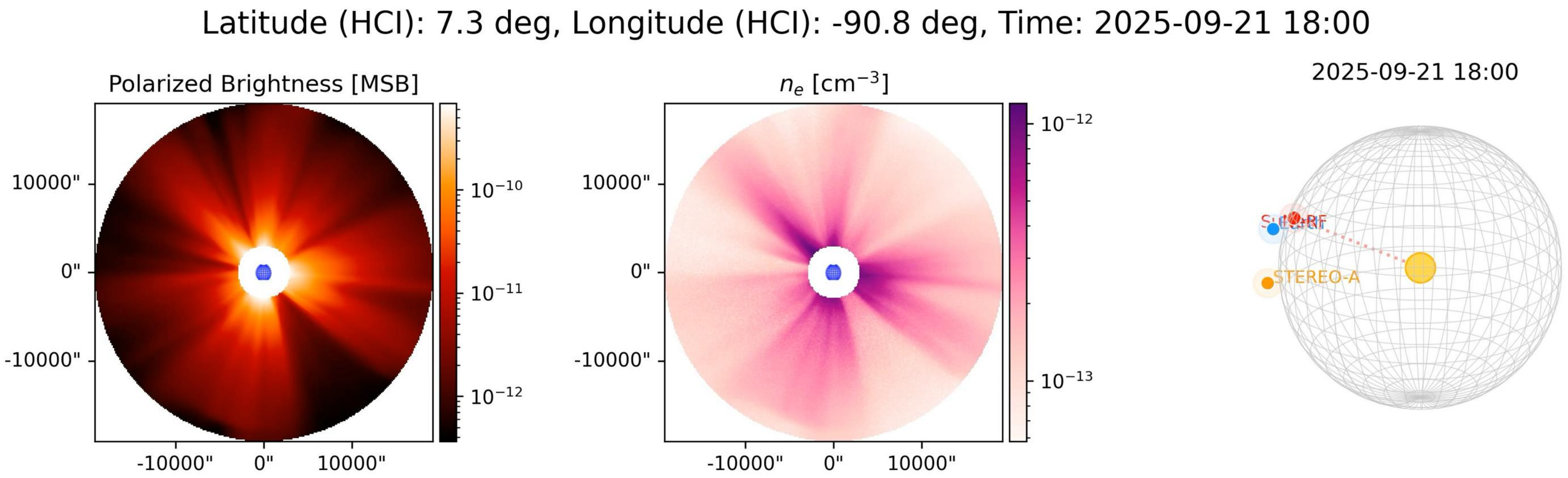

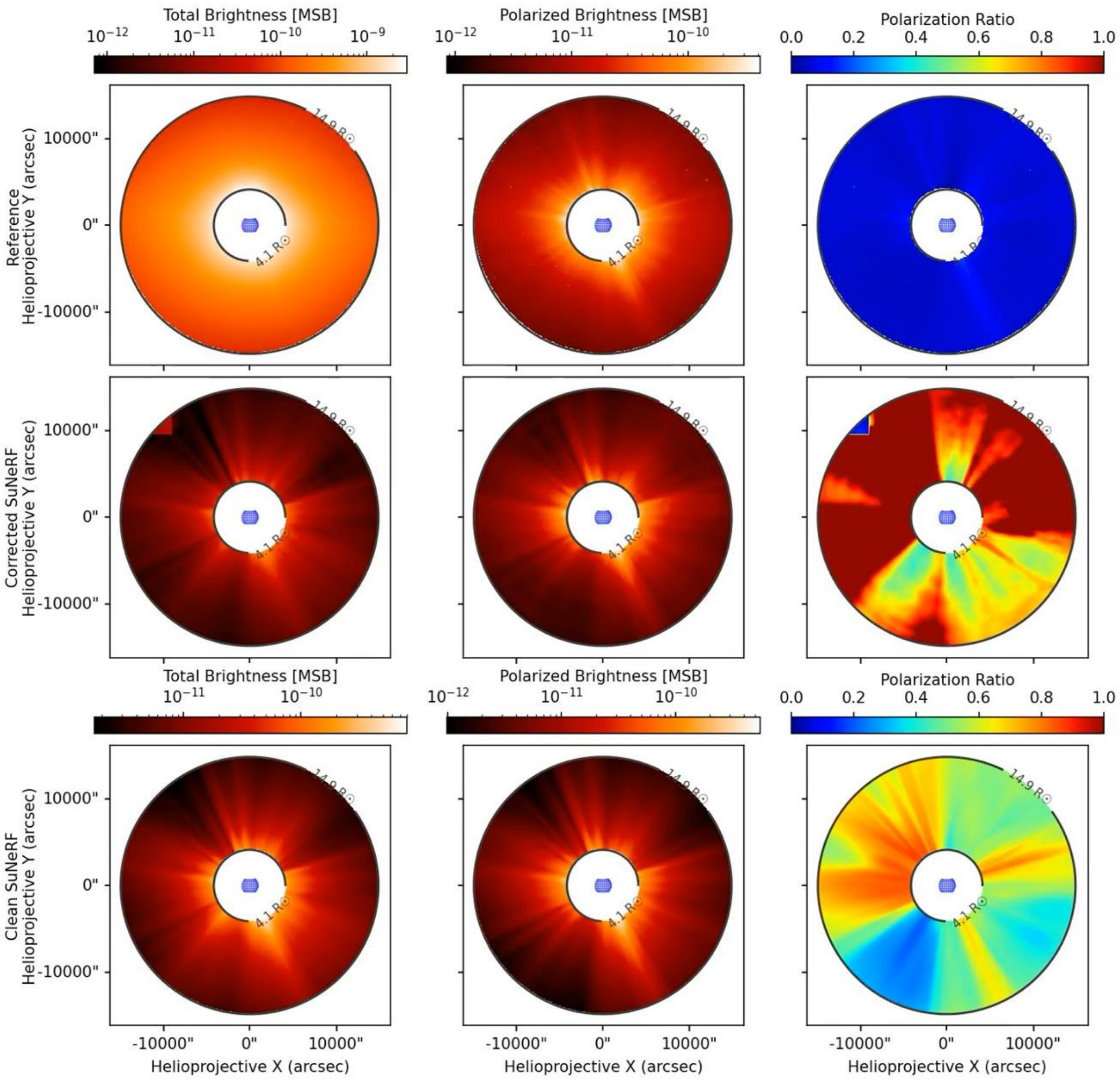
Total Brightness [MSB]
Polarized Brightness [MSB]
Polarization Ratio
Reference
Helioprojective Y (arcsec)
Corrected SuNeRF
Helioprojective Y (arcsec)
Clean SuNeRF
Helioprojective Y (arcsec)
Helioprojective X (arcsec)
14.9 R⊙
4.1 R⊙
10000"
0"
-10000"
0.0
0.2
0.4
0.6
0.8
1.0

Derived CME parameters – 2 viewpoints

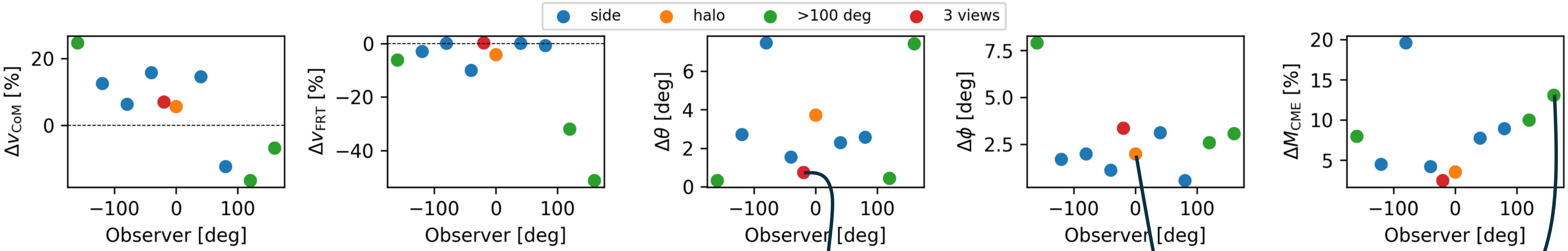

- CME parameters based on 2 observers from different viewpoints (60° separation) (0°=full halo CME)
- <100° separation to CME:
  - ΔVelocity (front): -3%
  - ΔMass: 8%
  - ΔLatitude: 3°
  - ΔLongitude: 2°

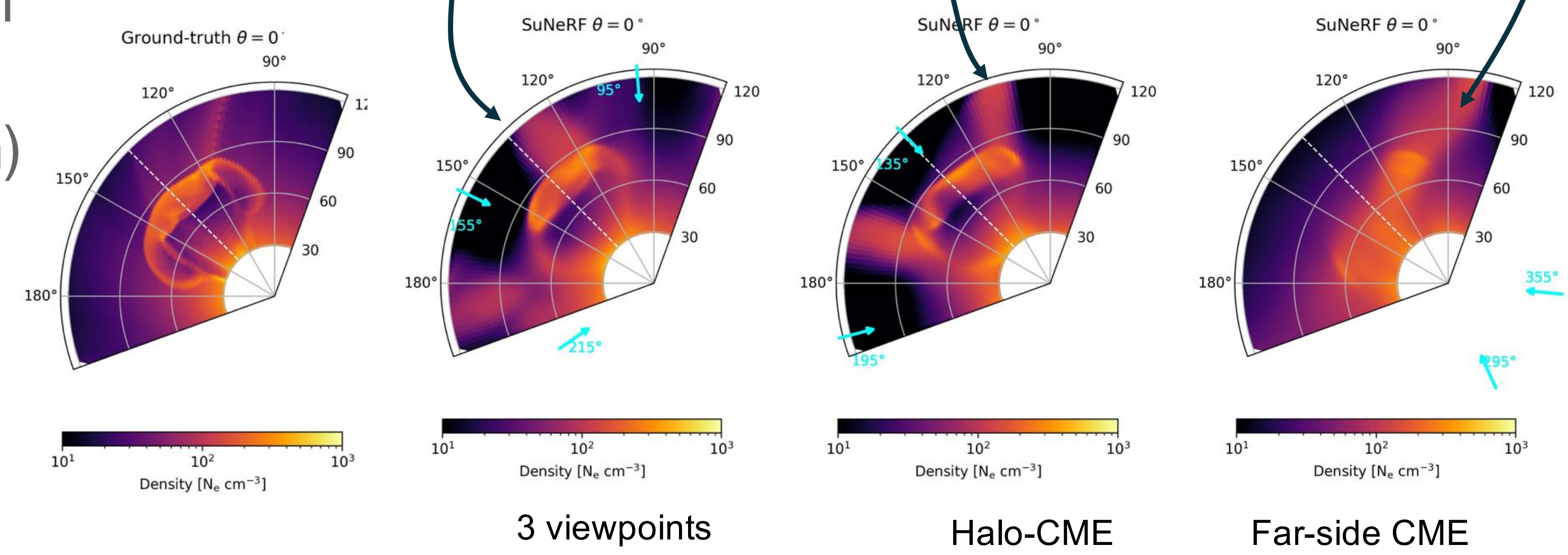

NSF | NCAR | NASA

Importance of Physics Constraints

- Physics constraints **improve consistency** of reconstructions
- Reconstructions without physics show:
  - Spurious drift of center-of-mass
  - Variable mass
  - Potential ghost trajectory
  - Fuzzy background

a) Slices through ecliptic plane
b) Evolution of CME parameters

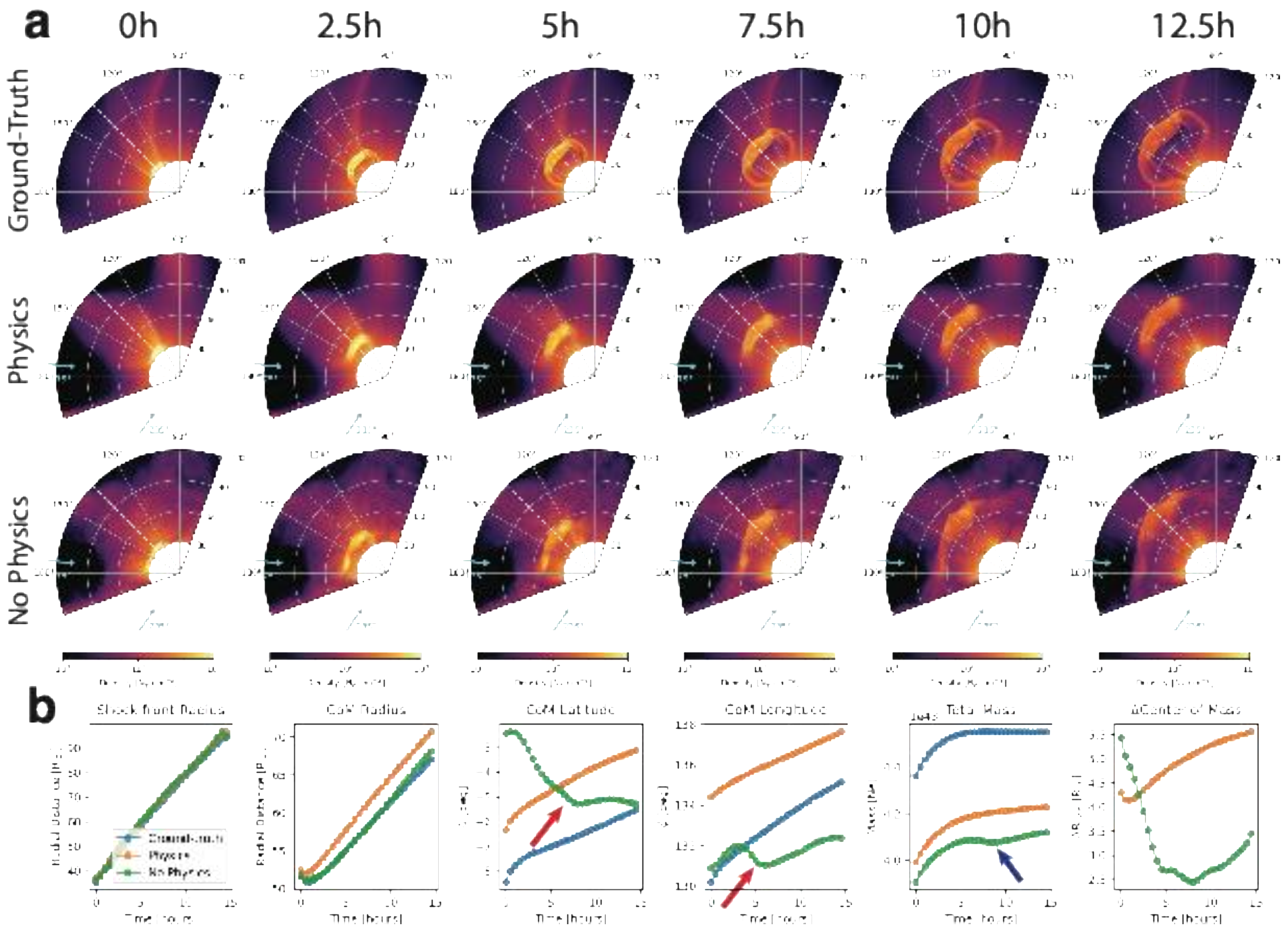

Tomographic reconstruction with Physics-Informed Neural Radiance Fields

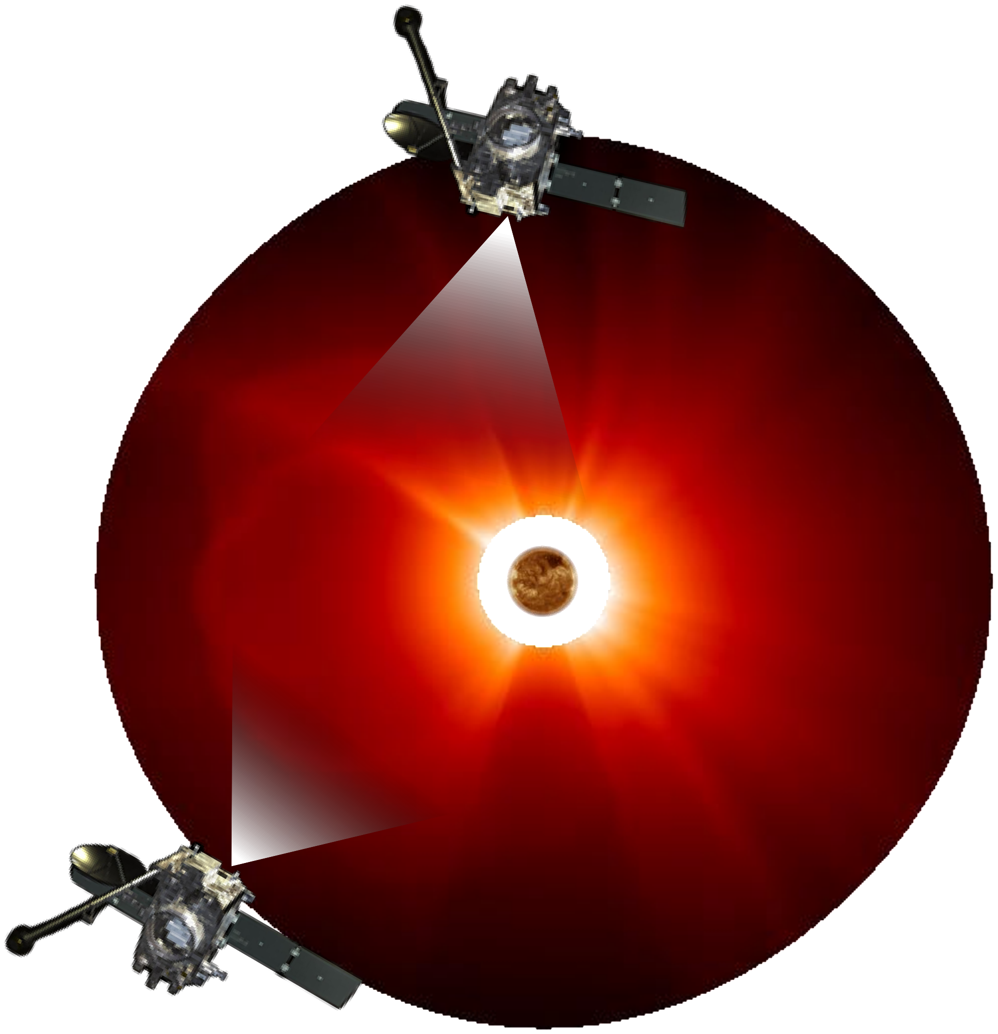

- Coronal observations are difficult to interpret
  - Human fitting can be **subjective**
    (e.g., triangulation, CGS reconstruction; Verbeke et al. 2022)
- **Tomography**: Use observations from **multiple viewpoints** to reconstruct the **3D plasma distribution** in the corona and heliosphere.

Tomographic reconstruction with Physics-Informed Neural Radiance Fields

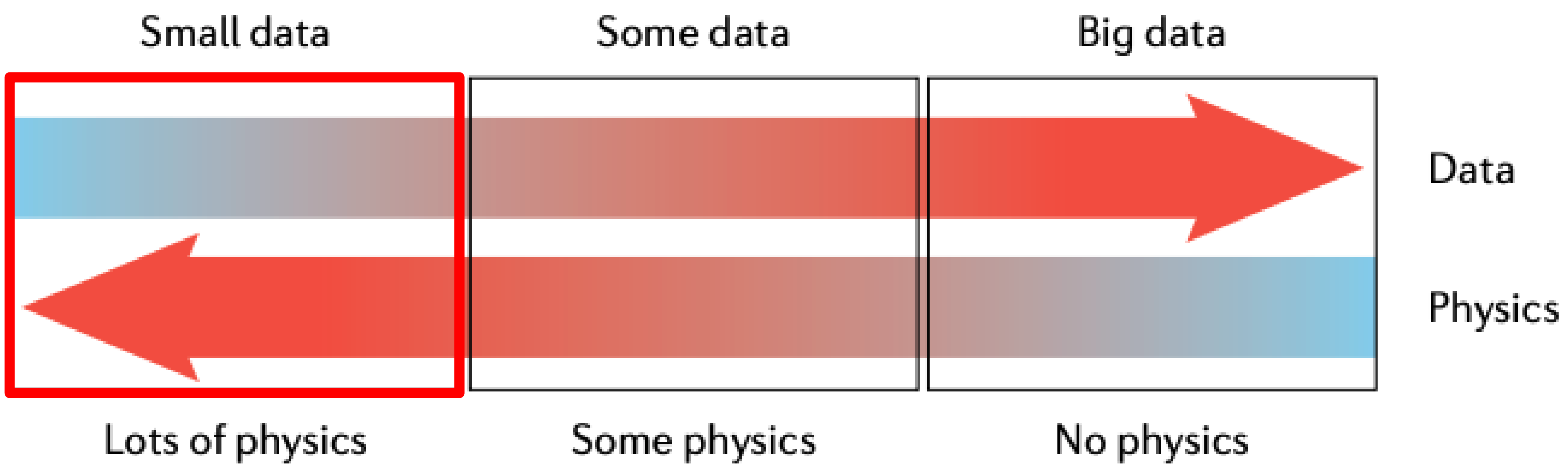

- Small data: known **physics** and **boundary condition**
- **Solver method** for **Partial Differential Equations** (PDEs)

→ Incorporate additional physics constraints to overcome limitations

- Neural network acts as function approximation of simulation/reconstruction volume

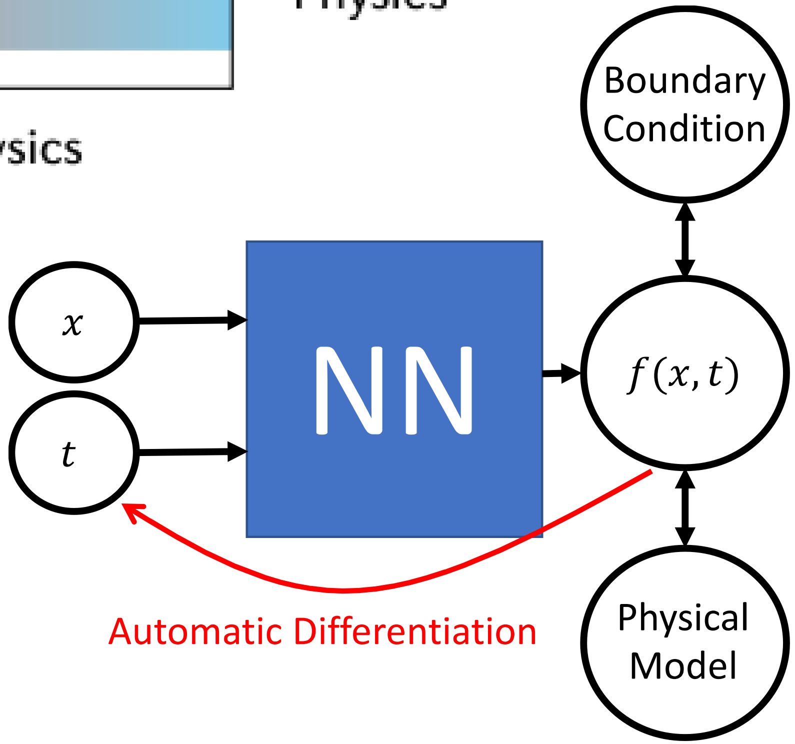

Tomographic reconstructions

Thomson Scattering

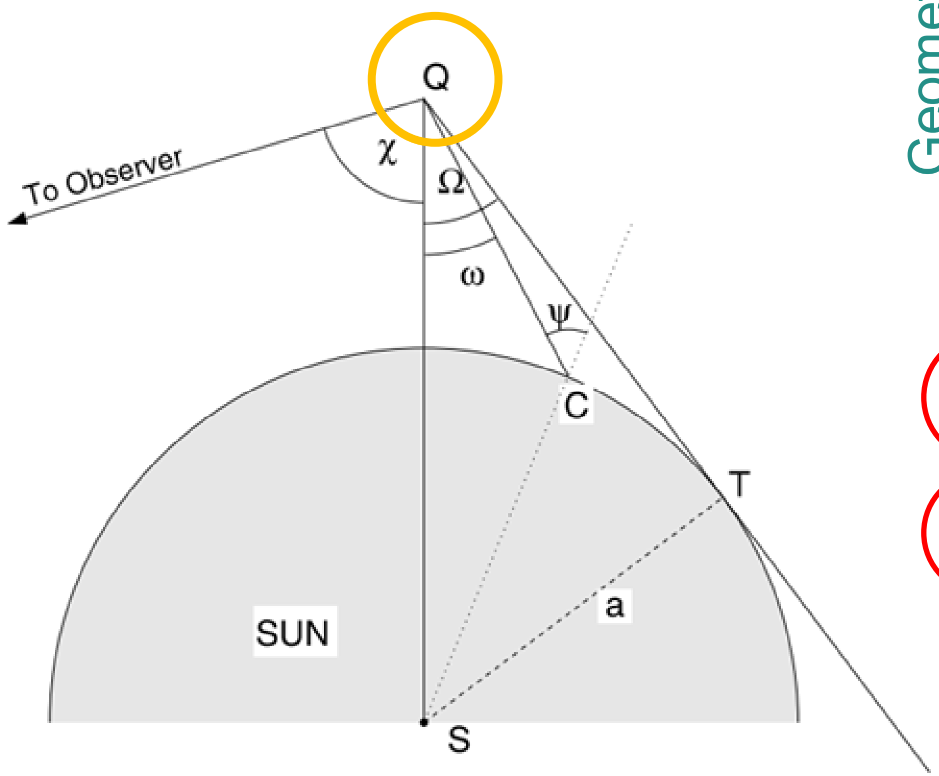

Howard, Timothy A., and S. James Tappin. "Interplanetary coronal mass ejections observed in the heliosphere: 1. Review of theory." *Space science reviews* 147 (2009): 31-54.

Geometry

$$A = \cos\Omega \sin^2\Omega,$$

$$B = -\frac{1}{8}\left[1 - 3\sin^2\Omega - \frac{\cos^2\Omega}{\sin\Omega}(1 + 3\sin^2\Omega)\ln\left(\frac{1+\sin\Omega}{\cos\Omega}\right)\right],$$

$$C = \frac{4}{3} - \cos\Omega - \frac{\cos^3\Omega}{3},$$

$$D = \frac{1}{8}\left[5 + \sin^2\Omega - \frac{\cos^2\Omega}{\sin\Omega}(5 - \sin^2\Omega)\ln\left(\frac{1+\sin\Omega}{\cos\Omega}\right)\right].$$

$$I_T = I_0 \frac{\pi\sigma_e}{2z^2}[(1-u)C + uD]$$

$$I_P = I_0 \frac{\pi\sigma_e}{2z^2}\sin^2\chi\,[(1-u)A + uB]$$

$$I_{tot} = 2I_T - I_P$$

Observed brightness depends on scattering **geometry**

Ghost trajectories can be unphysical solutions (DeForest et al. 2013)

Observed brightness and temporal evolution provides spatial information